Sliding Mode Control of Autonomous Under Water Vehicle

By

Muhammad Farhan

MEE153023

A thesis submitted to the

Department of Electrical Engineering

in partial fulfillment of the requirements for the degree of

MASTER OF SCIENCE IN ELECTRICAL ENGINEERING

Faculty of Engineering

Capital University of Science & Technology

Islamabad

May 2017

TO MY PARENTS AND BELOVED FAMILY

CERTIFICATE OF APPROVAL

The research work carried out in this report is certified to be done under the supervision of Prof. Aamer Iqbal Bhatti, at Capital University of Science & Technology, Islamabad.

Supervisor:

Prof. Aamer Iqbal Bhatti
Professor
Dept. of Electrical Engineering,
Faculty of Engineering
Mohammad Ali Jinnah University.

Co-Supervisor:

Dr. Waseem A Kamal

Imran Khan Yousafzai

CERTIFICATE OF CHANGES

This is to certify that Mr. Muhammad Farhan has incorporated all observations, suggestions and comments made by external examiner , internal examiner and thesis supervisor.

_____

Dr. Aamer Iqbal Bhatti
(Thesis Supervisor)

ACKNOWLEDGMENT

Firstly I am thankful to ALMIGHTY ALLAH for giving me the nerve, mental ability and health during the span of my work. I am grateful to Prof. Aamer Iqbal Bhatti for believing in me to work under his supervision. He steered me in the the direction which was the best for me. I am also grateful to Dr. Mansoor Ahmed for giving me the financial benefits through out the process of my MS degree.
I would also acknowledge Dr. Imran Khan yousafzai and Dr. Waseem Ahmed Kamal who's sincere suggestions always proved to be fruitful in the way of completing my thesis. I am thankful to Dr. Noor Khan, Dr. Fazl u Rehman and Dr Imtiaz Ali Taj for giving me the knowledge that proved to be helpful.

I am also thankful to all the members of CASPR (Control And Signal Processing Research) Group. Special thanks to my seniors Dr. Yasir Awais Butt, Mr. Armaghan Mohsin and Mr. Amin Akram. Also thanks Mr. Ali Arshad, Mr. Ghulam Murtaza, Mr. Raheel Anjum, Mr. Ahmed Yar, Mr. Muhammad Asghar, Mr. Syed Ussama Ali, Mr. Athar Hanif, Mr. Abdul Rehman Yasin, Mr. Zeeshan Babar, Mr. Rizwan Azam, Mr. Fahad Murad, Mr. Fahad Amin, Mr. Jamal Ahmed Bhatti, Mr. Farooq Saleem Mr. Farrukh Waheed, Mr Azmad Saeed, Mr Usman Zafar, Mr Nawaz sharif, Mr. Zohaib Latif, Mr. Abdul Waiz and Mr. Atif Adnan.

It would be an ultimate pleasure to acknowledge my Father, who taught me the patience, devotion and commitment, and my mother who is symbol of ultimate affection.

In the last but not the least, I am thankful to my friends Mr. Syed Tajamul Shah, Mr. Waqas Arif, Mr. Bismillah Jan, Mr. Sadam Hussain and all those who stood with me in my tough time.

DECLARATION

It is declared that this is an original piece of my own work, except where otherwise acknowledged in text and references. This work has not been submitted in any form for another degree or diploma at any other university or institution for tertiary education and shall not be submitted by me in future for obtaining any degree from this or any other University or Institution

Muhammad Farhan
MEE153023

May 2017

ABSTRACT

In the modern era Autonomous underwater vehicles are gaining importance for its major contribution in scientific, commercial and military underwater applications. To perform underwater task autonomous guidance and control system is needed.This report consists the mathematical modeling and trajectory control of the AUVs. The report covers a brief survey on available AUVs, sensors used in it and its application in defense and commercial areas. Kinematic and Dynamic equations are derived for the vehicle in 6 DOF motion. The vehicle can operate in six degree of freedom motion having a highly nonlinear dynamic equation.

The open loop simulations for KAMBARA AUV have been carried out using MATLAB/ SIMULINK for the experimental data available. A PID controller for depth, pitch, roll, steering and forward direction is designed for the vehicle using the knowledge of its EOM. SMC is also established for control of the Vehicle for the above mentioned DOF, the results are simulated with MATLAB. The performance of the designed controllers is evaluated by comparing results accomplished with SMC and PID.

Ocean currents are one of major cause in the disturbance of the AUV motion, it is therefore, important to add it to the dynamical EOM. The thesis includes the performance comparison of the designed controllers in the presence of ocean currents as well.

TABLE OF CONTENTS

LIST OF FIGURES

LIST OF TABLES

LIST OF ACRONYMS

PID	Proportional + Integral + Derivative
SMC	Sliding Mode Control
AUV	Autonomous Underwater Vehicle
ROV	Remotely Operated Vehicle
EOM	Equation of Motion
MBE	Multi Beam Echo sounder
SBP	Sub Bottom Profiles
SAS	Synthetic Aperture Sonar
SSS	Side Scan Sonars
CTD	Conductivity Temperature Density
ADCP	Acoustic Doppler Current Profiler
INS	Inertial Navigation system
IMU	Inertial Measurement Unit
DVL	Doppler Velocity Log
LBL	long Baseline
USBL	Ultra short baseline
MCM	Mines countermeasures
UXO	Unexploded Ordinance
SSAM	Small Synthetic Aperture Mine-hunter
LSG	Large Scale Gradiometer
BFF	Body Fixed Reference Frame
ERF	Earth Reference Frame

LIST OF SYMBOLS

Symbol	Description	Units
u	Surge velocity	m/s
p	Roll rate	rad/s
v	Sway velocity	m/s
q	Pitch rate	rad/s
w	Heave velocity	m/s
r	Yaw rate	rad/s
ψ	yaw angle in ERF	rad
x	Translation in ERF	m
X	Force in BFF along x	N
N	Moment along yaw in BFF	
θ	Pitch angle in ERF	rad
y	Translation in ERF	m
Y	Force in BFF along y	N
M	Moment along pitch in BFF	
ϕ	Roll angle in ERF	rad
z	Translation in ERF	m
Z	Force in BFF along z	N
K	Moment along roll in BFF	
W	Weight of vehicle	
B	Buoyancy force	
COG	Center of Gravity	
COB	Center of Bouyoncy	
I_x	inertia moment along x axis	
I_y	inertia moment along y axis	
I_z	inertia moment along z axis	
I_{xy}	product of inertia w.r.t x and y axis	
I_{xz}	product of inertia w.r.t x and z axis	
I_{yz}	product of inertia w.r.t y and z axis	

Chapter 1

INTRODUCTION

Unmanned Under Water Vehicles (UUVs) can be classified to two types

- Autonomous Under Water Vehicles(AUVs)
- Remotely Operated Under Water Vehicles (ROVs)

Remotely operated underwater vehicle are underwater robots that has a controller located above the surface of water. ROVs are controlled by person on surface through a cable connection. Power and control signals are transferred to the vehicle with the help of an umbilical cable also the sensor and video data is sent back to the operator through it. For missions which require autonomy the ROV is not preferred, it is convenient to use autonomous underwater vehicle. The Study is focused on the deriving the EOM and control of Autonomous Under Water Vehicles.

1.1 Autonomous Under Water Vehicles

AUVS are self-guided, pre-programmed vehicles with on-board sensors and computer [6]. Operator has no physical (cable) connections with the vehicle. The basic aim in designing the AUVs is to achieve a fully automatic, intelligent and decision making vehicle [11]. Missions or tasks are loaded to the AUV in form of instructions..

1.1.1 Basic Structure

AUVs Structure is designed to make its propagation smooth and easy in under water environment.The basic units of AUVs are

Propulsion unit The propulsion unit consists of thrusters and propellers responsible for the motion of the Vehicle under Water. Propulsion unit can have various thrusters which can provide thrust in the desired direction. Usually stepper motors are used for the rotation of the propellers. This Unit is the high Power consumption unit of the AUVs.

Hull Unit A water tight hull is designed to keep the electronics and other circuitry sensitive to water in it. The Hull is a water tight easily accessible unit, it is designed such that the components are easily adjustable and replaceable when required. The hull should be corrosion free as it will be used in deep sea and salty environment. Mostly found in spherical, cylindrical or ellipsoidal shape.

Power Unit It Consists of power generating and power distribution unit [6] [1]. Often sealed batteries are used for providing the power [11] while power is distributed to electrical components according to the requirement. Care is taken while selecting the power generating source with respect to size, cost and reliability.

Submerging The AUVs are often used under water rather than on the surface of water so Submerging is needed. Two kind of techniques are used or submerging of the vehicle which are:

Ballasting: This technique is used in static submarines. When AUVs are at the surface of the water dry air is filled in the ballast tanks that gives density of AUV less than the surrounding water. In order to sink the vehicle the tanks are filled with water so that its density increases than the surrounding water and AUVs starts submerging [12]

Thrusters: This technique is used in dynamic submarines. The thrusters point downwards to push the submarines into the water. This technique is inefficient in terms of power consumption.

1.1.1.1 Sensors used in AUV

Various Sensors are used for AUVs based on specified tasks the AUV is designed for. The most common sensors used are discussed here.

Multi Beam Echo sounder

MBE are used for mapping seabed by emitting sound waves. It also calculate water depth by calculating the time taken by sound waves to bounce back from seabed towards the receiver.

Sub Bottom Profiles

Sub Bottom Profiles (SBP) has the same working principle as MBE but with greater penetration power. It produces a pulse of 10khz-30khz capable of penetrating through the seabed, SBP are ideal for identification layers of sediment under sea floor.

Synthetic Aperture Sonar

Synthetic Aperture Sonar (SAS) gives higher resolution images as compared to other sonars by combining number of acoustic pings. SAS illuminates the same spot with several pings to create a high resolution image.

Side Scan Sonars

Side Scan Sonars (SSS) are used for conducting marine archeological surveys. Mostly used for detetion of objects on the seafloor.

Conductivity Temperature Density

For measuring the essential physical properties of sea water like conductivity, temperature and Density CTD is one of the important tool. It gives a precise comprehensive charting of distribution and variation of water temperature, salinity and density.

Acoustic Doppler Current Profiler

The speed of sea water is measured with ADCP. It uses doppler effect of sound waves to measure speed in an entire water column.

Turbidity Sensor

This sensor measures the haziness of water by calculating the amount of light scattered by suspended particles in water.

1.1.1.2 Navigation System used for AUV

Autonomous under water vehicle are fully autonomous vehicle which results a challenging task for navigating the vehicle in a highly unstructured environment. In order to perform the missions accurately the AUV must follow the path as specified to it as close as possible. Maintaining Position accuracy of AUV is a primary challenge in navigation of AUV. Different methods for navigation of AUV are discussed.

Inertial Navigation

Dead Reckoning techniques uses the vector information i.e direction and speed to estimate the current position from a known starting point. This technique is not preferred as the position accuracy is dependent upon the vector information.

Inertial Navigation system (INS) uses accelerometers and gyroscopes for measuring the acceleration and position of the AUV without any external reference. In inertial navigation system Inertial Measurement Unit (IMU) is the main component. Inertial navigation system are subjected to integration drift. Small errors in acceleration are integrated to constantly can results greater error in position of AUV. For improvement Doppler Velocity Log (DVL) sonar is used for longer missions. DVL has the limitation to be used only near the sea bed. DVL and INS are combined to improve performance but with the same limitation that it has a drift which may be reduced by resetting the drift to external reference point.

Acoustic Navigation

In acoustic navigation the underwater vehicle is tracked and navigated by means of acoustic distances. The technique uses acoustic beacons in the mission area of the AUV. The two common type of techniques used are long baseline (LBL) and Ultra short baseline (USBL). The LBL uses at least two beacons which are placed

on the seafloor. The acoustic signals sent by AUV are returned by these beacons and using the knowledge of beacons position, speed of sound wave and time taken by it the AUV can determine its current position. In USBL only a single beacon is used which is attached to surface ship through which AUV can determine the current location. LBL and USBL are range limited and are operated in a specific range.

Geophysical navigation

Observable Physical features are used in Geophysical navigation to observe AUV position. Usually the area map is provided to the AUV. Geophysical navigation is dependent on the features available and extraction feature ability of the system from the sensor data.

Figure 1.1 shows a typical structure for AUV.

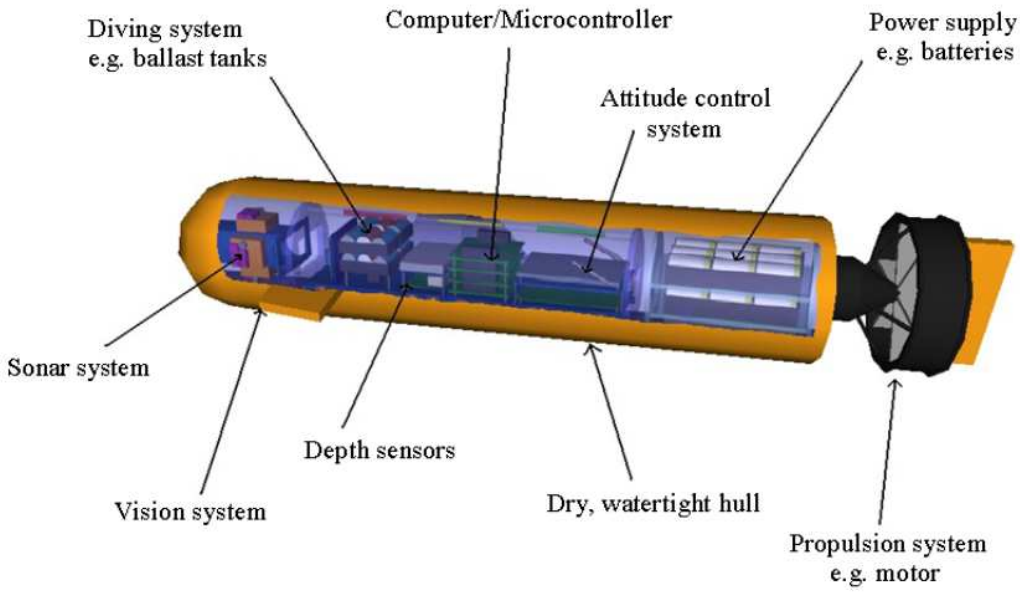

FIGURE 1.1: AUV basic structure [1]

1.1.2 Basic Operation

AUVs are pre-programmed with a specific missions in form of instructions. Geographical location, desired propellers movement, maps, intelligence of obstacle avoidance and much more are loaded in it through instructions. As mentioned before that AUV do not have any cable interface but it can have a telecommunication link with the operator for real time data interchange and change in missions according to the requirement.

General Block Diagram for AUV

A generalized block diagram for an AUV can be as given in Figure 1.2

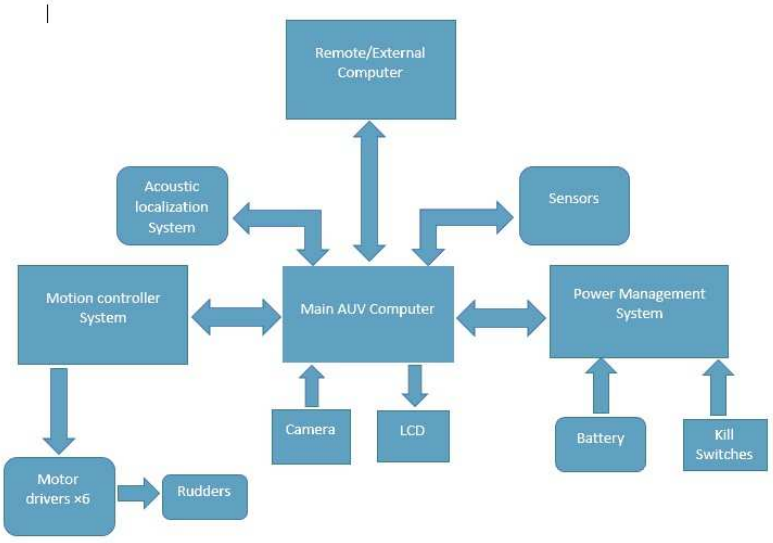

FIGURE 1.2: General block diagram for AUV

1.2 Types of AUVs

1.2.1 REMUS

Remote Environmental Monitoring Units (REMUS) vehicles found its use in vast applications like navy, hydrography and marine research. REMUS AUVs are designed at Woods Hole Oceanographic Systems Lab n U.S.

- REMUS are Low Cost AUVs
- Designed by Oceanographic system lab
- Consists of propellers and wings to steer and dive

REMUS Models

REMUS vehicles differ by size, depth, endurance and payload sensor configuration. Uses acoustic navigation. Data is recorded using different installed sensors. The sensor information and Application of REMUS AUV is given with respective model

1.2.1.1 REMUS 100

REMUS 100 is a light weight AUV (37 kg) designed to operate in coastal environment. It has an ability of operating at 100 meters underwater. It has a diameter of 0.19m and length 1.6m [13]. REMUS 100 can be configured according to the requirement of the mission [8]. Easy and simple Vehicle Interference Program (VIP) with two man portable capability. Can be used for any sub-sea application with capability of having the required sensors.

Applications

1. Defense

FIGURE 1.3: REMUS 100 AUV [2]

- Area search and surveillance
- Mine counter measures (MCM)

2. Commercial

- Emergency response
- Asset location
- Pipeline survey

Sensor

Various sensors can be used with Remus 100 including temperature sensor, salinity sensor, SSS, sensor for sound speed and water velocities.

1.2.1.2 REMUS 600

REMUS 600 is AUV with a diameter of 0.32, length 3.2m and weight 272kg. More payload capability with increased battery capacity. It has 45 hours mission duration and depth range up to 600m. Sensors aided are[8].

Sensors

- Small Synthetic Aperture Minehunter (SSAM) : high resolution
- LSG (Large Scale Gradiometer) : large area search and target localization

FIGURE 1.4: Remus 600 AUV [2]

1.2.1.3 REMUS 3000

It has the same size as REMUS 600 but increased payload and depth range. REMUS 3000 is constructed of titanium and used for under water mapping and imaging.

Sensors

- Dual edged side scan sonars
- Navigation system coupled with GPS and LBL acoustic navigation to increase accuracy

1.2.1.4 REMUS 6000

It has a deeper depth range (6000 m) and wide range of Autonomous under water operation. Configurable according to the customers required sensors.

1.2.1.5 REMUS Shark-cam

Special type of REMUS Vehicle with ability to track and locate marine animal like white shark. It is equipped with Camera and scientific instrumentation.

1.2.1.6 REMUS Tunnel Inspection

A 45 miles section of Delaware Aqueduct was checked for leaks by REMUS Tunnel Inspection in 2004 [14].

1.2.2 HUGIN AUVs

Hugin Autonomous under water vehicles started in 1990s for civilian and military applications. Kongsberg maritime and Norwegian Defence Research Establishment are its developers. IT has depth capacity up to 6000m with completion of about 600,000 line kilometre survey. Hugin AUVs are commercially operated in Europe, Africa, America, Asia and Australia [14].

Sensors

- MBE: Multibeam echo sounders
- SBP: Sub Bottom Profiles
- SSS: Side Scan Sonars
- SAS: Synthetic Aperture Sonars
- CTD: Conductivity Temperature Density
- Turbidity sensors
- Methane Sensor
- Acoustic Doppler Current Profiler (ADCP)

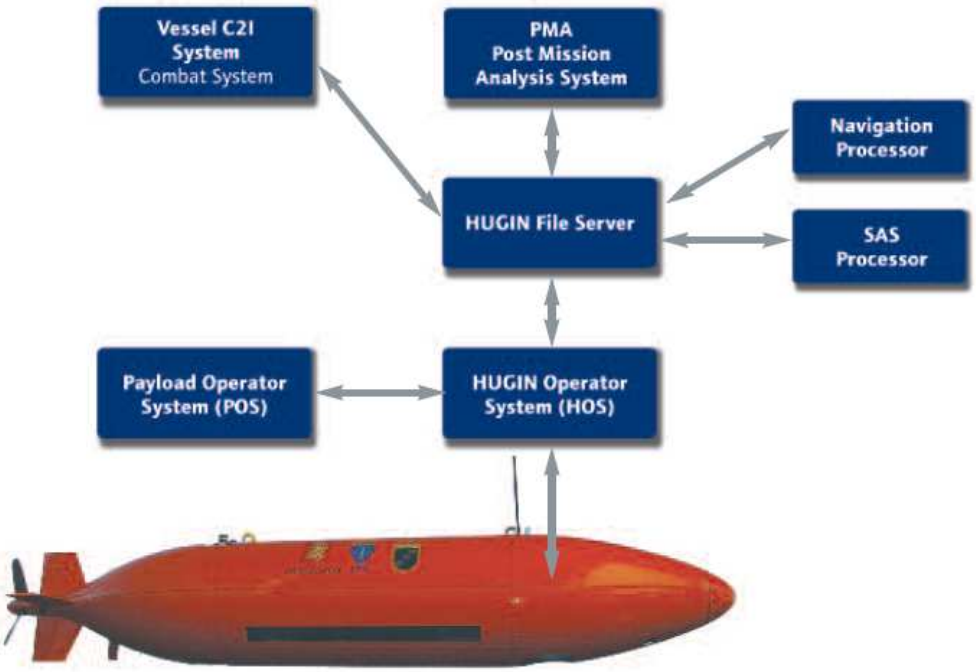

FIGURE 1.5: Hugin AUV [2]

Applications

- Mines countermeasures (MCM)
- Object detection through high resolution SAS.
- Rapid Environmental Assessment (REA)
- Intelligent Surveillance & Reconnaissance (ISR)
- Environmental Monitoring

Available models are:

1.2.2.1 Hugin 1000

It has depth capability of 1000m and work capability 24 hours with a speed of 4 knots.

1.2.2.2 Hugin 3000

Hugin 3000 AUV has a diameter of 1 meter with a dive range upto 3000 meters underwater. Its speed range is 4 knots and 60 hours work time.

1.2.2.3 Hugin 4500

It has a depth capability of 4500 meter with 30 % increased battery capacity and more payload sensors.

1.2.3 Munin AUV

Munin are High position and navigation Capable AUVs. It consists of Autonomous pipe tracking software for survey and inspection. Munin have depth capability 600-1500 meters with high payload sensors. It has a diameter of 0.34m, length 2.6-3.5 meters and weight 300kg.

Applications

- Geophysical Survey
- Pipe-lining Survey
- Environmental Monitoring
- Hydrography (Route Survey)
- Search and Recovery

1.2.4 Sea Gliders AUV

Sea gliders are developed by Kongberg maritime. It uses wings and changes in buoyancy to achieve forward motion, does not have any electrically driven propellers as shown in 1.7. Adjustable blast is used for orientation control. Sea gliders

FIGURE 1.6: MUNIN AUV [3]

has a depth capability of max 1000m having a saw tooth like trajectory[13].

Sensors

- Current profilers
- Conductivity Temperature Density (CTD)
- Dissolve oxygen Sensors
- Photo-synthetically Active Radiation (PAR)

Applications

- Surveillance

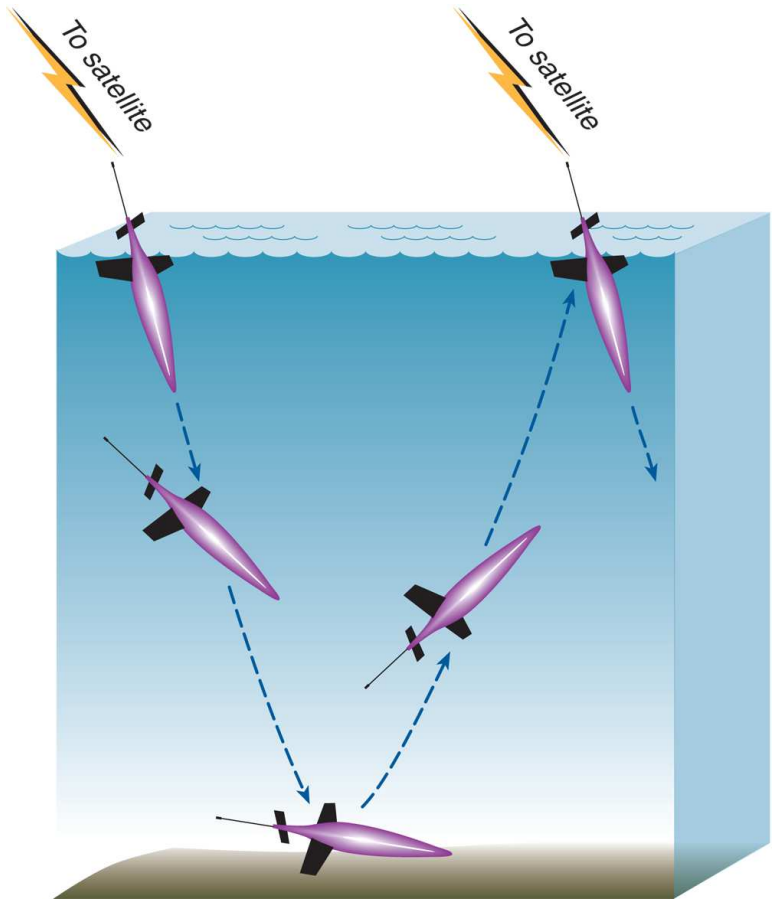

FIGURE 1.7: underwater motion of Sea glider [4]

- Environmental monitoring
- Oceanography
- Fisheries research

1.2.5 Blue-fin Robotics

Blue-fin robotics deals with development of AUVs and other technologies related for commercial, defence and scientific use. Their models include

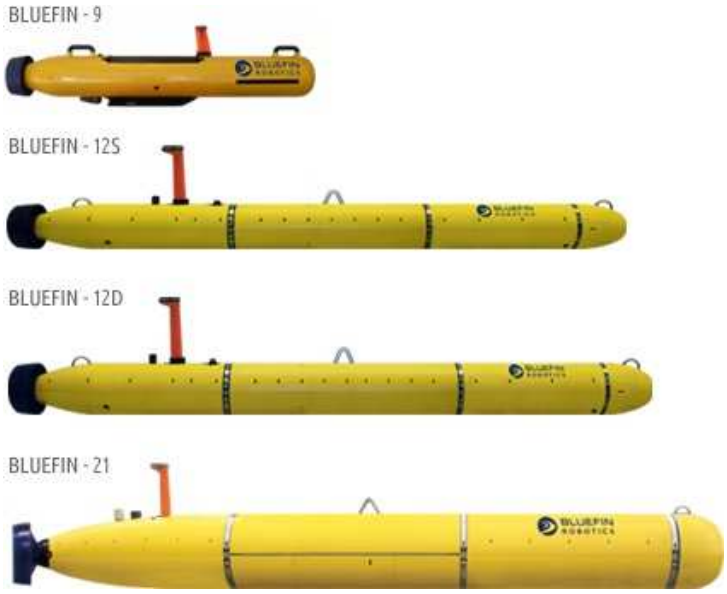

FIGURE 1.8: Different available models of Bluefin AUVs [5]

1.2.5.1 blue-fin 9

It is a light weight AUV with accurate navigation and rapid turnaround time from missions ($\leq$ 15 minutes). Bluefin 9 provides accurate navigation by using IMU with GPS,DVL, CT and a compass.

Applications

- Environmental protection and monitoring
- Rapid Environmental Assessment (REA)
- Intelligent Surveillance & Reconnaissance (ISR)
- Mine Counter Measures (MCM)
- Unexploded Ordinance

1.2.5.2 blue-fin 12s

Blue-fin 12S is capable of carrying multiple payload sensors with rapid turnaround time. It consists of swappable payload sections and battery modules so can be configured within the field. This AUV is air shippable and ideal for remote operation with max depth range of 4500 meters. It uses IMU combined with GPS,DVL,SVS and a compass.

Applications

- Mine Counter Measures (MCM)
- Unexploded Ordinance (UXO)
- Oceanography
- Archeology and Exploration

1.2.5.3 blue-fin 21

The depth range is increased in Bluefin 21 with multiple payload and sensors. It uses INS with USBL to provide accurate navigation. Applications are same as Bluefin 12S [15].

1.2.6 AUV Explorer

Explorer is a low cost operating AUV which is owned and operated by French research agency. The depth range is 300-600 meters underwater. In spring 2010 it covered 1000 meters of travelling under ice covered water.

1.2.7 Iver 2-580 s Standard AUV

It is a single person operated AUV built by ocean server. It is a light weight (19 kg) and low cost operating AUV with depth capability of 100 meters.

Sensors

- Side Scan Sonars (SSS)
- Multi Beam Sonars (MBS)
- Acoustic Doppler Current Profiler (ADCP)
- Conductivity Temperature Density (CTD)
- Acoustic Modem

Chapter 2

EXISTING CONTROL APPROACHES

The main problems associated with control of AUVs are unmodeled dynamics, parametric uncertainties along with nonlinear and coupled dynamics. By studying literature of Unmanned under water Vehicles (AUV & ROV) it is observed that research study related with 'control' has a broad range. Listed below are the three main categories these studies can be classified to.

Motion Control: it is related to the response of AUV for its input and the stability of vehicle.

Mission Control: deals with achieving the pre-defined mission of AUV installed on its board computer.

Formation control: deals with the organization control of numerous underwater vehicles amongst them.

The figure 2.1 shows the schematic explanation of studies on motion control [6].

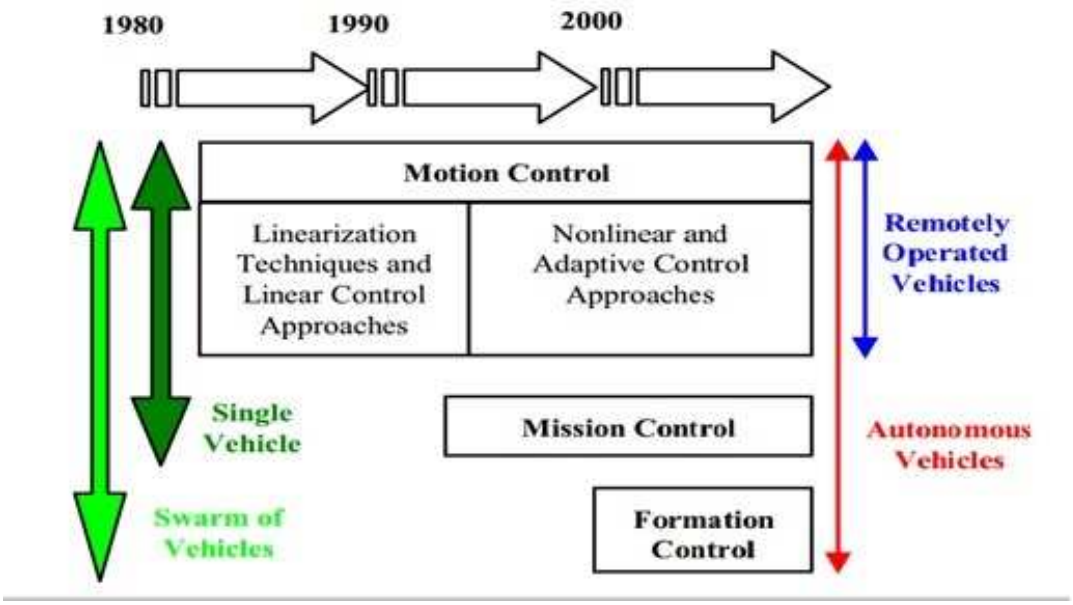

FIGURE 2.1: Studies on motion control [6]

2.1 Control problems in AUVs:

Control simply means to achieve the behavior of the system according to our desire, and the mechanism used to achieve the goal is called control system. Once the mathematical modeling of the AUVs has been accomplished the main problem to tackle is to design a controller for the vehicle which can handle the disturbances and uncertainties accurately while achieving the desired task (position and velocity) [6] [11]. Underwater vehicles controlling has always been a difficult area because of the dynamics of underwater. Researchers have proposed many techniques for controlling and stabilizing the AUVs. This research will be focused to design an accurate controller for AUVs to achieve the autonomy

2.1.1 Stability of underwater vehicles

Stability for underwater vehicles is defined as its ability to return to the equilibrium state once disturbed without use of any corrective action like use of control surfaces

(thruster, motor etc.) [9]. Further we have two types of stability which can be defined for Underwater Vehicles

2.1.2 Open Loop Stability (Control Fixed)

It is the stability of the vehicle investigated when the control surfaces are fixed and does not vary.

2.1.3 Closed Loop Stability

It is the stability of the vehicle investigated when the control surfaces are varying, this requires to consider the dynamics of control system in stability analysis.

2.2 Motion Control of Underwater Vehicles

To achieve better and robust performance in presence of environmental disturbances closed-loop control system is required. Sensors and navigation data are used to feedback in closed loop system.
In 1990s control problem was mainly tackled by decoupling the 6 DOF motion into three separate Subsystems for speed, diving and steering control.
For the control and stability of Autonomous under Water Vehicles numerous methods are used in literature. Two kinds of approaches can be used:

2.2.1 Linear Control Systems

A full state feedback control for diving control of AUV has been applied by [11] . The technique is applied to USM AUV. Authors uses pole placement method to calculate the gain matrix k. Paper provides good results with assumption that all states are available. This assumption results in costly control and due to increase of sensors the probability of error increase.
In [12] author Provides a feedback linearization for 6 DOF equation of motion for AUV. The author decouples the 6 DOF equation of motion into six 2nd order

deferential equation. The stabilization is achieved by adding a PD compensator to each if the subsystem. This linear method is much dependent upon precise modeling and ability to cancel out non linearities.

In [16] state feedback linearization technique has been adopted by the authors, using linear Quadratic Regulator approach to find out the feedback matrix. In order to satisfy the optimality this technique is utilized. It controls the four basic motions u, w, θ and ψ. The designed controller lack the disturbance rejection feature.

Computed torque control based PID tracking controller was adopted by [8]. The computed torque needs the parameters to be known precisely. Also optimal control is not guranteed by PID as AUV has highly nonlinear behaviour [6]. PID controller for yaw, depth and surge speed control of AUV is also used in [13]. The author uses a decoupled linear model.

A P-D set point controller is implemented in [15] by considering the AUV dynamics and applied to fully actuated systems. Lyapunov based argument is taken to guarantee the stability of AUV.

Optimal control for kinematic model of AUV is provided in [17]. Linear Quadratic Gaussian (LQG) technique is used. This method is suitable for uncertain linear system. The Author linearizes the system and transform it into chain form.

In [18] system identification (SI) is used to get the model through input/output data utilizing an LQG controller. SI provides accurate and short time models in short period of time saving to go through complex mathematical modeling techniques.

2.2.2 Nonlinear control Systems

The technique considers the nonlinear dynamical model of AUV by considering the uncertainties associated with the 6 DOF motion.

[19] uses SMC for Autonomous Underwater Vehicle. The non linearities in the dynamical model of AUV are tackled using this robust technique. The stability of

control system is achieved by lyponove theory. The problem with use of SMC is the chattering issue. [20] Uses two techniques for nonlinear control of AUVs which are Adaptive Passivity-based control scheme and hybrid (Adaptive & sliding) controller. The hybrid controller contains sign function (switching) to compensate the uncertainties in the input matrix & online parameter estimation are also provided by the controller. The author simulates for horizontal motion of the AUV.
[1] Uses a smooth second order real twisting control for lateral dynamics control of AUV. 3 DOF is controlled considering an under actuated control problem. The model imprecision is avoided by considering nonlinear control scheme

A chattering free HOSM controller is provided in [21] for AUV Taipan. Author compares the results with classical SM control. Techniques used are Twisting and super twisting.
Adaptive nonlinear control for depth control of AUV is accomplished by [22] the author breaks the assumption of small pitch angle. Back stepping is used to design an adaptive nonlinear controller. A PID & Fuzzy logic controller is used in [23] to track the horizontal under water telecommunication cable. Fuzzy logic controller requires a fully known dynamics of the controlled system which is one of its limiting factor.
The trajectory tracking and path following problem of AUV is addressed in [24]. System considered is under actuated system and author uses hybrid control technique. The problem not addressed here is noise and presence of disturbances like wind, wave & ocean currents.

2.2.3 SMC and PID schemes for AUV

In the thesis two control schemes are addressed , PID and SMC. The control schemes are simulated for the KAMBARA AUV, the prototype of KAMBARA is

used as a reference to get a dynamical model for its simulation. SMC is one of the robust non-linear control recently existing.

[25] addresses depth and steering control of AUV using SMC in open control platform , the authors uses a linearized model for the corresponding state control. The stability of other states is not discussed. [14] Utilizes PID & Sliding Mode Control for linearized model of AUV. The technique is used for depth and heading control of MUUTC (Manta Type Unmanned under Water Test Vehicle) and results are compared with NPS (Naval postgraduate School) AUVII. PID lack to handle the uncertainties accurately while sliding mode control can provide enough robustness to uncertainties, The authors uses the linearized dynamical model for the controller designing.

The 6 DOF equation of motion is linearized under several equilibrium points in [26]. The authors derives a control law using SMC for the yaw steering control.

A non linear SMC is derived for the non-linear dynamical model of AUV in [27]. The designed SMC shows the accurate tracking of the velocities for AUV. In [28] The depth of Hovering autonomous underwater vehicle (HAUV) is controlled using robust sliding mode control.

2.2.4 Proposed Control Scheme

Going through the literature it has been depicted that a robust control is required not only in depth displacement of AUV but in all 6 DOF for AUV. The stability of the vehicle is required to be analyzed in the 6 DOF motion. It is also important to check the vehicle performance in presence of the ocean currents, which are the main cause to effect the motion of AUV. A novel SMC for the AUV is established in the 6 DOF motion. The results are to be compared with the designed PID controller.

Chapter 3

MATHEMATICAL MODEL FOR AUV

The 6 DOF equation of motion for Autonomous Underwater Vehicle is completely derived in this chapter. The chapter also covers the model of ocean currents to be included in the dynamic model of the AUV. KAMBARA AUV is used as a prototype and its open loop simulations are performed using MATLAB/ SIMULINK and the results are discussed.

3.1 AUV Kinematics

Kinematics deals with study of motion of body without considering cause of motion. The motion of AUV is explained with the help of two reference frames, BFF which is denoted by(X_0, Y_0, Z_0) and ERF denoted by (X, Y, Z). Figure below shows the coordinates required for study of AUV.

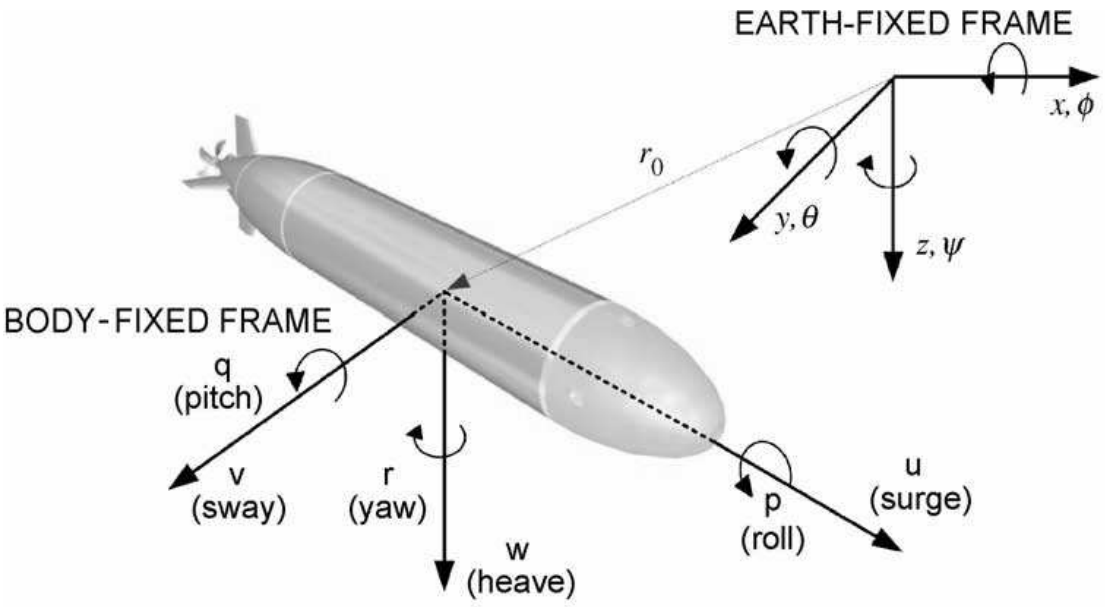

FIGURE 3.1: Inertial frame and vehicle body frame [7]

DOF	Motion	Forces / moments	velocity	translation / orientation
1	Surge	X	u	x
2	Sway	Y	v	y
3	Heave	Z	w	z
4	Roll	K	p	ϕ
5	Pitch	M	q	θ
6	Yaw	N	r	ψ

TABLE 3.1: SNAME notation used for marine vehicles

3.1.1 AUV Coordinate and Frame of Reference

AUV has a 6 DOF motion. It is convenient to take the body-fixed frame origin and the center of gravity (COG) to be the same. For AUV the ERF is presumed to be inertial which results in no effect on the motion of AUV by the earths motion. The translation and orientation are expressed in the inertial frame, while the linear and angular velocities are expressed in the body frame for AUV. The general motion of AUV can be given by the notations given by SNAME (1950) as:

$$\eta = \begin{bmatrix} \eta_1 & \eta_2 \end{bmatrix} = \begin{bmatrix} x & y & z & \phi & \theta & \psi \end{bmatrix}^T \tag{3.1}$$

$$V = \begin{bmatrix} V_1 & V_2 \end{bmatrix} = \begin{bmatrix} u & v & w & p & q & r \end{bmatrix}^T \tag{3.2}$$

$$T = \begin{bmatrix} T_1 & T_2 \end{bmatrix} = \begin{bmatrix} X & Y & Z & K & M & N \end{bmatrix}^T \tag{3.3}$$

Here translation and orientation in earth reference frame is represented by η.The linear and angular velocities in the body reference frame are given by V. While the vector of forces and moments acting upon the AUV is given by T [9][1][29].

3.1.2 Transformation of Co-ordinates

In order to transform properties of one Reference frame to other a relation between the two reference frame is required. Euler angles are used for the two type of

transformation as discussed:

3.1.2.1 Linear velocity transformation

linear velocity transformation is given by:

$$\dot{\eta_1} = J_1(\eta_2)v_1 \tag{3.4}$$

here $\dot{\eta_1}$ is the linear velocity transformed to earth reference frame through transformation matrix $J_1(\eta_2)$ .The inverse transformation is given by $v_1 = J_1^{-1}(\eta_2)\dot{\eta_1}$, the equation represents transformation of linear velocities from earth inertial frame to body fixed frame of reference.

Simple Rotation

If we have two rigid bodies A and B then the motion of B relative to A will be said to as simple rotation if the orientation of axis of rotation (L) remain unchanged relative to rigid bodies A and B [9][30]. if we have a vector 'a' fixed in A and vector 'b' fixed in B then b can be represented in terms of a by:

$$b = cos\beta a + (1 - cos\beta)\lambda\lambda^T a - sin\beta\lambda \times a$$

by using the xyz-convention for rotation of coordinates, the following transformation matrices are yielded.

$$C_{x,\phi} = \begin{bmatrix} 1 & 0 & 0 \\ 0 & cos\phi & sin\phi \\ 0 & -sin\phi & cos\phi \end{bmatrix}, C_{y,\theta} = \begin{bmatrix} cos\theta & 0 & -sin\theta \\ 0 & 1 & 0 \\ sin\theta & 0 & cos\theta \end{bmatrix} C_{z.\psi} = \begin{bmatrix} cos\psi & sin\psi & 0 \\ -sin\psi & cos\psi & 0 \\ 0 & 0 & 1 \end{bmatrix}$$

these matrices satisfy the following properties

$$det(C) = 1; CC^T = C^T C = I, C^-1 = C^T$$

The transformation matrix $J_1(\eta_2)$ can be calculated by combining rotation matrices as calculated above. If $X_3Y_3Z_3$ coordinate system is obtained by translating inertial coordinate system XYZ, such that the origin of XYZ is same as that of body fixed frame . Coordinate system $X_3Y_3Z_3$ is than rotated yaw angle ψ, followed by rotation at pitch angle θ and finally a rotation at roll angle ϕ to get body fixed coordinate system $X_0Y_0Z_0$ as shown in Figure 3.2 The rotation sequence is written as:

$$J_1(\eta_2) = C^T_{z,\psi} C^T_{y,\theta} C^T_{x,\phi}$$

$$J_1(\eta_2) = \begin{bmatrix} cos\psi cos\theta & -sin\psi cos\phi + cos\psi sin\theta sin\phi & sin\psi sin\phi + cos\psi cos\phi sin\theta \\ sin\psi cos\theta & cos\psi cos\phi + sin\phi sin\theta sin\psi & -cos\psi sin\phi + sin\theta sin\psi cos\phi \\ -sin\theta & cos\theta sin\phi & cos\theta cos\phi \end{bmatrix}$$

3.1.2.2 Angular velocity transformation

Transformation matrix given by $J_2(\eta_2)$ is used to transform the body fixed angular velocity to earth reference frame. The relation is give by is given by:

$$\dot{\eta_2} = J_2(\eta_2) v_2 \tag{3.5}$$

In order to get the transformation matrix we use orientation of body fixed frame with respect to earth fixed reference frame which is given as:

$$v_2 = \begin{bmatrix} \dot{\phi} \\ 0 \\ 0 \end{bmatrix} + C_{x,\phi} \begin{bmatrix} 0 \\ \dot{\theta} \\ 0 \end{bmatrix} + C_{x,\phi} C_{y,\theta} \begin{bmatrix} 0 \\ 0 \\ \dot{\psi} \end{bmatrix} = J_2^{-1}(\eta_2) \dot{\eta_2}$$

which gives:

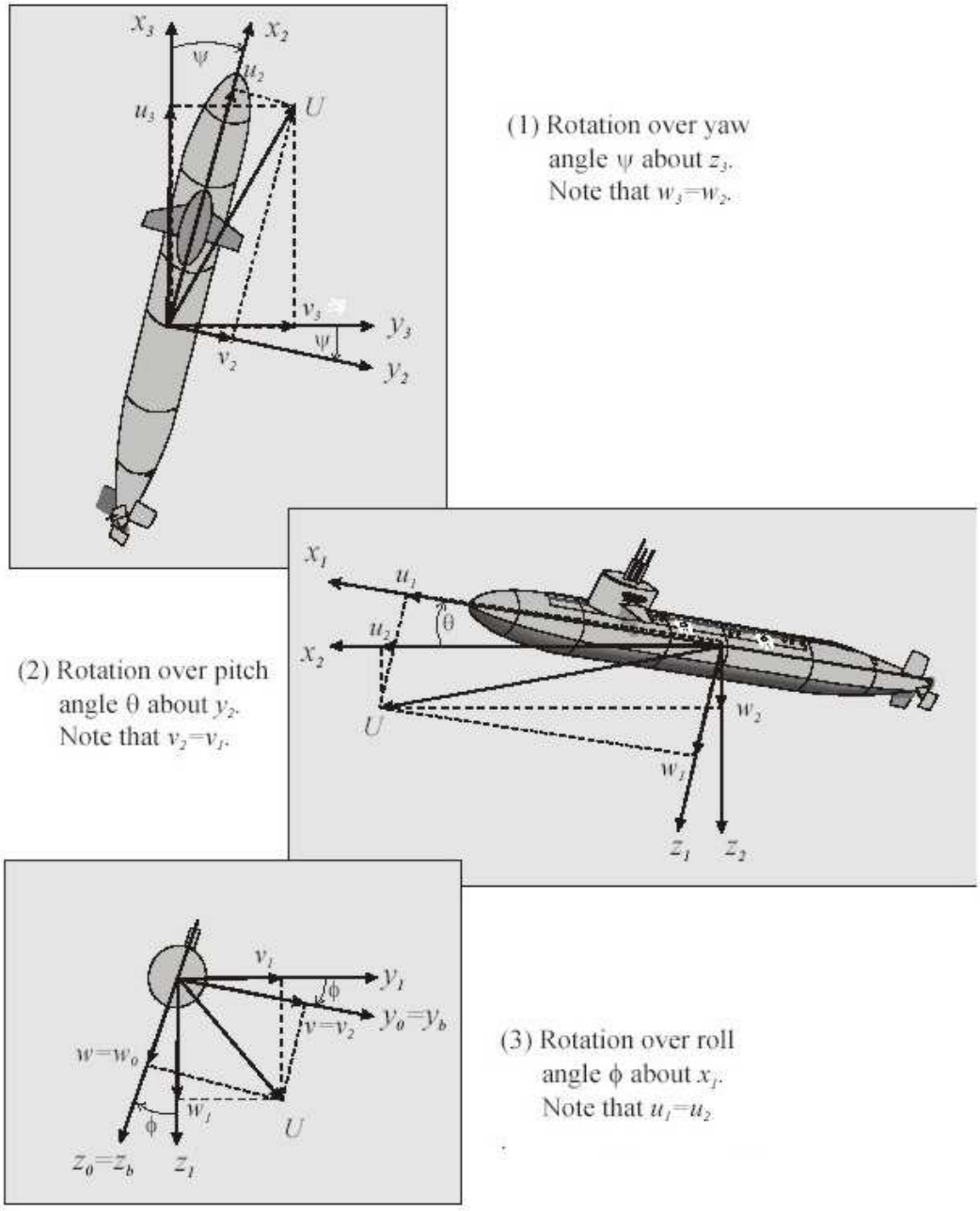

FIGURE 3.2: Rotation Sequence according to xyz-convention

$$J_2^{-1}(\eta_2) = \begin{bmatrix} 1 & 0 & 0 \\ 0 & cos\phi & cos\theta sin\phi \\ 0 & -sin\phi & cos\theta cos\phi \end{bmatrix}$$

By taking the inverse transformation we get

$$J_2(\eta_2) = \begin{bmatrix} 1 & sin\phi tan\theta & cos\phi tan\theta \\ 0 & cos\phi & -sin\phi \\ 0 & sin\phi/cos\theta & cos\phi/cos\theta \end{bmatrix}$$

The overall kinematic model can than be given by

$$\begin{bmatrix} \dot{\eta_1} \\ \dot{\eta_2} \end{bmatrix} = \begin{bmatrix} J_1(\eta_2) & 0_(3 \times 3) \\ 0_(3 \times 3) & J_2(\eta_2) \end{bmatrix} \begin{bmatrix} v_1 \\ v_2 \end{bmatrix} \tag{3.6}$$

3.2 Equation of Motion of AUV

To derive the equation of motion of the AUV it is important to know the factors which affect the dynamics of AUV. Discussed below are the factors that affects the motion of AUV.

3.2.1 Factors Affecting Motion of AUVs

1. **Buoyancy & Gravitational forces**

   force exerted on body equal to the volume of water it displaces is called the buoyant force. weight (W) and Buoyant (B) are collectively known as

hydrostatic forces. Hydrostatic forces are critical in destabilizing the AUV. If

- W > B , Object sink
- W < B , Object float [1]

For submerged bodies stability the COB should always be above the COG. Also for a stable AUV the COB and COG is aligned , any misalignment in both will result in a moment which disturb the stability of AUV. AUV having the same COG and COB is called a neutrally buoyant AUV.

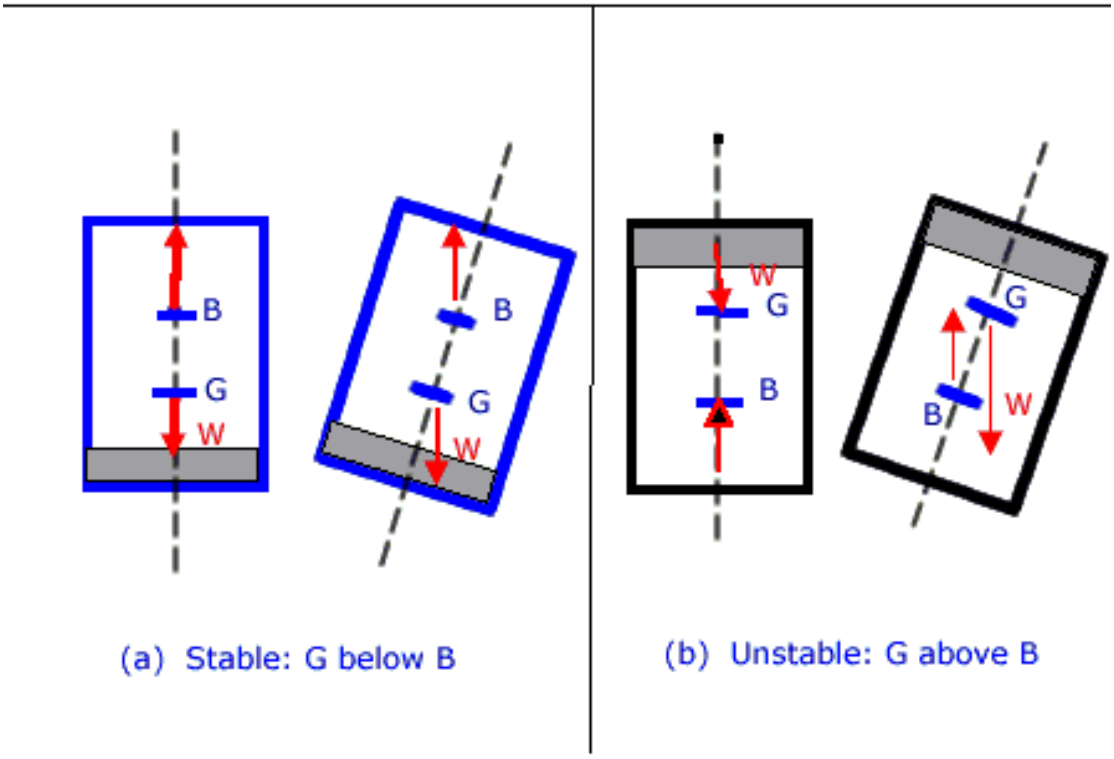

FIGURE 3.3: a) Stable position of a submerged body b) Unstable position of a submerged body [8]

2. **Coriolis Forces**

Coriolis force/ effect is phenomena in which a moving object is deflected relative to a rotating frame of reference and it is applied in a perpendicular direction to the body. Coriolis force is applied in opposite direction of the

rotation of rotating reference frame.

3. **Added Mass**

   Added mass are pressure-induced forces and moments as a result of forced harmonic motion of the body. There are no incidents waves but the forced motion of the body results in outgoing waves. This forced motion results in oscillating fluid pressures on the body surface. The resulting forces and moments on the body are found out by integration of fluid pressure forces over the body

   Added mass terms are related to vehicle shape, volume, acceleration and mass [31] [32] [33]

4. **Hydrodynamic damping**

   Forces acting on body due to velocity of surrounding fluid and fluid displaced by the body are called hydrodynamic damping forces. it results in coupling and non-linearity in AUV. the forces included are Drag and Lift

   - *Drag*: Force in opposite direction to velocity, as a result of fluid
   - *Lift*: In perpendicular direction to the AUV velocity

   Both of these forces resist the motion of AUV [1] [8]

3.2.2 Equation of motion

The EOM can be deducted using Newton Second law of motion.

Assumptions while deriving:

1. The body of vehicle is rigid
2. ERF is assumed to be inertial

The assumption of the vehicle to be rigid is important as it eradicates the forces due to individual elements as distance between elements is always constant and second eliminates forces due to earth motion. The formula needed to derive equation of motion for an arbitrary origin in a local Body fixed coordinate system is

$$\dot{c} = \mathring{c} + \omega \times c$$

where $\dot{c}$ is time derivative in the inertial frame and $\mathring{c}$ is time derivative in BFF $X_oY_oZ_o$ (moving).

so we can write,

$$\dot{\omega} = \mathring{\omega} + \omega \times \omega = \mathring{\omega}$$

the relation shows that the angular acceleration is same in body and earth reference frames .

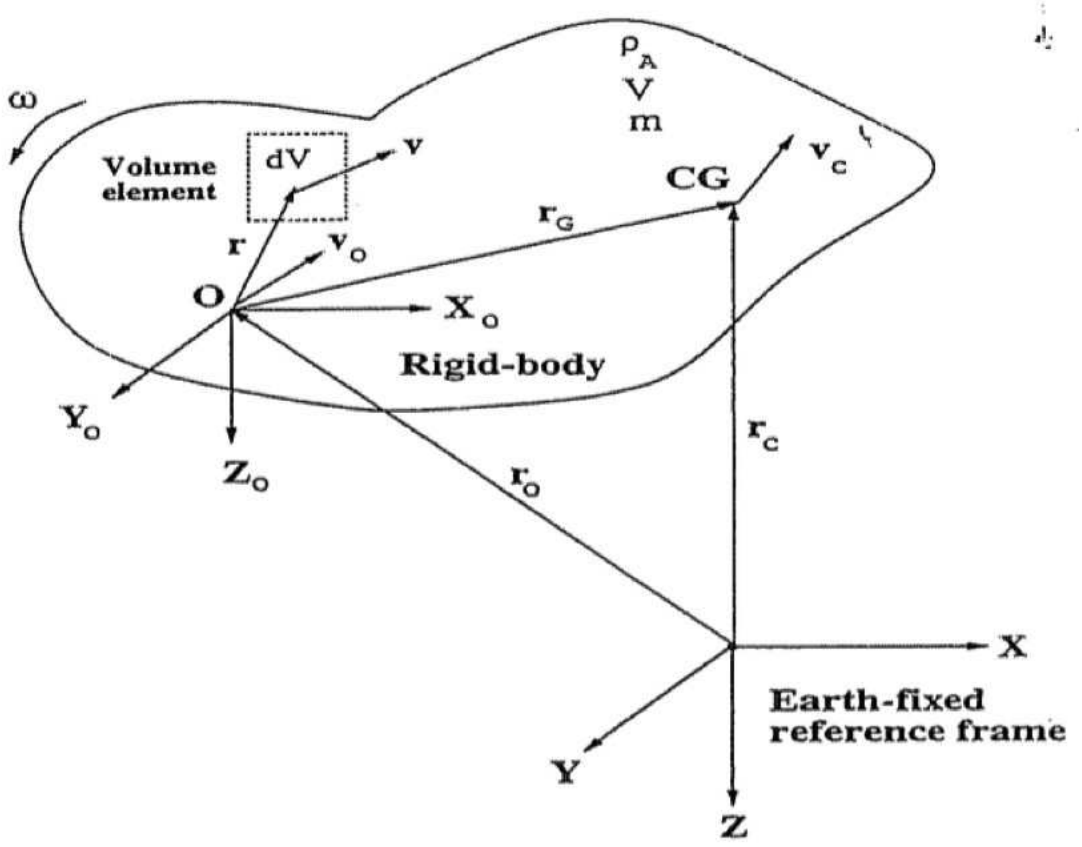

FIGURE 3.4: The earth-fixed non-rotating reference frame XYZ and body-fixed rotating reference frame $X_oY_oZ_o$ [9]

3.2.2.1 Translational motion

The relation to derive the translation motion for AUV is given by

$$\dot{P}_c = f_c \tag{3.7}$$

$$\dot{P}_c = mv_c \tag{3.8}$$

where P_c is the linear momentum referred to the vehicles COG, $\dot{P}_c$ is its time derivative, velocity of the COG is given by v_c , f_c is the external force and m is the mass of the vehicle.

In Figure 3.3:

O= BFF origin

CG= COG

r, r_o, r_g, r_c= Position Vectors

v_o, v_c, v= Velocity Vectors

ω= Angular velocity of rigid body w.r.t Earth fixed coordinate

From Figure 3.3 we have

$$r_c = r_o + r_G$$

velocity of the COG is :

$$v_c = \dot{r_c} = \dot{r_o} + \dot{r_G}$$

from Figure we get $v_o = \dot{r_o}$ and for rigid body we have $\mathring{r_G} = 0$

then we can write,

$$\begin{aligned} \dot{r_G} &= \mathring{r_G} + \omega \times r_G \\ &= \omega \times r_G \end{aligned}$$

hence,

$$v_c = v_o + \omega \times r_G$$

acceleration vector is given by:

$$\dot{v_c} = \dot{v_o} + \dot{\omega} \times r_G + \omega \times \dot{r_G}$$

$$\dot{v_c} = \mathring{v_o} + \omega \times v_o + \mathring{\omega} \times r_G + \omega \times (\omega \times r_G)$$

substituting values in equation (3.8) gives

$$f_o = m(\mathring{v_o} + \omega \times v_o + \mathring{\omega} \times r_G + \omega \times (\omega \times r_G)) \tag{3.9}$$

which is the required translational motion of the vehicle. If the origin of body frame and COG are taken the same then the equation is simplified as

$$f_c = m(\mathring{v_c} + \omega \times v_c) \tag{3.10}$$

3.2.2.2 Rotational motion

The angular momentum is given by

$$h_c = I_c \omega \tag{3.11}$$

$$\dot{h_c} = m_c \tag{3.12}$$

here I_c is the inertia tensor matrix, ω is the angular velocity and m_c are the moments refereed to body COG.

The absolute angular momentum about the origin O is given by

$$h_o = \int_v r \times v \rho_A dV$$

here r is the position vector of particle as shown in Figure 3.3 , v is the velocity and ρ_A is the mass density of particle.

By time differentiating the above equation

$$\dot{h_o} = \int_v r \times \dot{v}\rho_A dV + \int_v \dot{r} \times v\rho_A dV \tag{3.13}$$

Looking to Figure 3.3 we get:

$$\dot{r_o} + \dot{r}$$

$$\dot{r} = v - v_o +$$

Equation (3.13) will become after substituting the above values

$$\dot{h_o} = m_o + \int (v - v_o) \times v\rho_A dV$$

$$\dot{h_o} = m_o - v_o \times \int_v v\rho_A dV$$

$$\dot{h_o} = m_o - v_o \times \int_v \dot{r} + v_o\rho_A dV$$

$$\dot{h_o} = m_o - v_o \times \int_v \dot{r}\rho_A dV \tag{3.14}$$

As distance from Origin of the body to COG for a rigid body is $r_G = 1/m \int_v r\rho_A dV$

Now,

$$m\dot{r_G} = \int_v \dot{r}\rho_A dV$$

$$m(\omega \times r_G) = \int_v \dot{r}\rho_A dV$$

replacing this in equation (3.14)

$$\dot{h_o} = m_o - v_o \times m(\omega \times r_G)$$

$$\dot{h_o} = m_o - mv_o \times (\omega \times r_G) \tag{3.15}$$

Absolute angular momentum about origin is given by [9] [7]:

$$h_o = \int_v r \times v\rho_A dV$$

$$h_o = \int_v r \times v_o\rho_A dV + \int_v r \times (\omega \times r)\rho_A dV$$

here

$$\int_v r \times v_o \rho_A dV = \int_v r \rho_A dV \times v_o$$
$$\int_v r \times v_o \rho_A dV = m r_G \times v_o$$

and

$$\int_v \times(\omega \times r)\rho_A dV = I_o \omega$$

equation (3.13) becomes:

$$h_o = I_o + m r_G \times v_o$$

Assuming I_o is constant differentiating the equation:

$$\dot{h_o} = I_o \dot{\omega} + m(\dot{r_G} \times v_o + r_G \times \dot{v_o})$$
$$\dot{h_o} = I_o \dot{\omega} + m(\mathring{r_G} + \omega \times r_G \times v_o) + m(r_G \times \mathring{v_o} + \omega \times v_o)$$
$$\dot{h_o} = I_o \dot{\omega} + m(\omega \times r_G \times v_o) + m(r_G \times \mathring{v_o} + \omega \times v_o)$$
$$\dot{h_o} = I_o(\mathring{\omega} + \omega \times \omega) + m(\omega \times r_G) \times v_o + m r_G \times (\mathring{v_o} + \omega \times v_o)$$

$$\dot{h_o} = I_o \mathring{\omega} + \omega \times (I_o \omega) + m(\omega \times r_G) \times v_o + m r_G \times (\mathring{v_o} + \omega \times v_o) \tag{3.16}$$

using $(\omega \times r_G) \times v_o = -v_o \times (\omega \times r_G)$ and comparing equation (3.15) & (3.16) results in:

$$m_o = I_o \mathring{\omega} + \omega \times (I_o \omega) + m r_G \times (\mathring{v_o} + \omega \times v_o) \tag{3.17}$$

here I_o is the inertia tensor matrix with the property of Symmetric and Positive Definite while m is the mass of AUV.

$$I_o = \begin{bmatrix} I_x & -I_{xy} & -I_{xz} \\ -I_{yx} & I_y & -I_{yz} \\ -I_{zx} & -I_{zy} & I_z \end{bmatrix}$$

with I_x, I_y, I_z are moments of inertia about X_o, Y_o, Z_o and $I_{xy} = I_{yx}, I_{xz} = I_{zx}, I_{yz} = I_{zy}$ are the products of inertia. If we choose Body Origin coincide with COG of the vehicle then simplified equation will be given by.

$$I_c\mathring{\omega} \ + \omega \times (I_c\omega) = m_c$$

using SNAME notations

$f_o = \tau_1 = [X, Y, Z]^T$

$m_o = \tau_2 = [K, M, N]^T$

$v_o = V_1 = [u, v, w]^T$

$\omega = V_2 = [p, q, r]^T$

$r_G = [x_G, y_G, z_G]^T$

By applying these notation to equation (3.9) and (3.17) we get final EOM as [9, 7]

$$\begin{aligned}
m\left[\dot{u} - vr + wq - x_G\left(q^2 + r^2\right) + y_G\left(pq - \dot{r}\right) + z_G\left(pr + \dot{q}\right)\right] &= X \\
m\left[\dot{v} - wp + ur - y_G\left(r^2 + p^2\right) + z_G\left(qr - \dot{p}\right) + x_G\left(qp + \dot{r}\right)\right] &= Y \\
m\left[\dot{w} - uq + vp - z_G\left(p^2 + q^2\right) + x_G\left(rp - \dot{q}\right) + y_G\left(rq + \dot{p}\right)\right] &= Z
\end{aligned} \tag{3.18}$$

$$\begin{aligned}
I_x\dot{p} + \left(I_z - I_y\right)qr - \left(\dot{r} + pq\right)I_xz + \left(r^2 - q^2\right)I_yz + \left(pr - \dot{q}\right) \\
+m\left[y_G\left(\dot{\omega} - uq + vp\right) - z_G\left(\dot{v} - wp + ur\right)\right] = K \\
I_y\dot{q} + \left(I_x - I_z\right)rp - \left(\dot{p} + qr\right)I_xy + \left(p^2 - r^2\right)I_zx + \left(qp - \dot{r}\right)I_yx \\
+m\left[z_G\left(\dot{u} - vr + wq\right) - x_G\left(\dot{w} - uq + vp\right)\right] = M \\
I_z\dot{r} + \left(I_y - I_x\right)pq - \left(\dot{q} + rp\right)I_yz + \left(q^2 - p^2\right)I_xy + \left(rp - \dot{p}\right)I_zx \\
+m\left[x_G\left(\dot{v} - wp + ur\right) - y_G\left(\dot{u} - vr + wq\right)\right] = N
\end{aligned} \tag{3.19}$$

Where first three equations represents translational motion and the last three equations are representing rotational motion of the AUV.

3.2.3 Dynamic model of AUV

To formulate control algorithms and to be able to perform simulation the dynamic model for AUV can be given by [9][7] [34][35]

$$M\dot{V} + C(V)V + D(V)V + g(\eta) = \tau \tag{3.20}$$

where,

M= inertia matrix (Added mass included)

C(V)= Coriolis and centripetal matrix

D(V)= Damping matrix

g(η)= vector of gravitational & buoyant forces

τ= Control input vector (6×1)

3.2.3.1 Mass and Inertia Matrix

The mass and inertia matrix consists of mass and added mass terms of the Autonomous underwater vehicle where M= M_A + M_{RB} M is a 6×6 matrix, M_A is added mass, M_{RB} is inertia and mass matrix respectively
The rigid body mass matrix is given by

$$M_{RB} = \begin{bmatrix} mI_{3\times3} & -mS(r_G) \\ mS(r_G) & I_o \end{bmatrix} = \begin{bmatrix} m & 0 & 0 & 0 & m_{zG} & -m_{yG} \\ 0 & m & 0 & -m_{zG} & 0 & -m_xG \\ 0 & 0 & m & m_{yG} & -m_{xG} & 0 \\ 0 & -m_{zG} & m_{yG} & I_x & -I_{xy} & -I_{xz} \\ m_{zG} & 0 & -m_{xG} & -I_{yx} & I_y & I_yz \\ -m_{yG} & m_{xG} & 0 & -I_{zx} & -I_{zy} & I_z \end{bmatrix} \tag{3.21}$$

If center of gravity and origin of AUV are chosen to coincide with each other and the body is assumed to be symmetric in all three planes then the matrix is simplified to:

$$M_{RB} = \begin{bmatrix} m & 0 & 0 & 0 & 0 & 0 \\ 0 & m & 0 & 0 & 0 & 0 \\ 0 & 0 & m & 0 & 0 & 0 \\ 0 & 0 & 0 & I_x & 0 & 0 \\ 0 & 0 & 0 & 0 & I_y & \\ 0 & 0 & 0 & 0 & 0 & I_z \end{bmatrix} \tag{3.22}$$

The hydrodynamic added mass terms are modeled as:

$$M_A = \begin{bmatrix} A_{11} & A_{12} \\ A_{21} & A_{22} \end{bmatrix} = \begin{bmatrix} X_{\dot{u}} & X_{\dot{v}} & X_{\dot{w}} & X_{\dot{p}} & X_{\dot{q}} & X_{\dot{r}} \\ Y_{\dot{u}} & Y_{\dot{v}} & Y_{\dot{w}} & Y_{\dot{p}} & Y_{\dot{q}} & Y_{\dot{r}} \\ Z_{\dot{u}} & Y_{\dot{v}} & Y_{\dot{w}} & Y_{\dot{p}} & Y_{\dot{q}} & Y_{\dot{r}} \\ K_{\dot{u}} & K_{\dot{v}} & K_{\dot{w}} & K_{\dot{p}} & K_{\dot{q}} & K_{\dot{r}} \\ M_{\dot{u}} & M_{\dot{v}} & M_{\dot{w}} & M_{\dot{p}} & M_{\dot{q}} & M_{\dot{r}} \\ N_{\dot{u}} & N_{\dot{v}} & N_{\dot{w}} & N_{\dot{p}} & N_{\dot{q}} & N_{\dot{r}} \end{bmatrix} \tag{3.23}$$

where SNAME (Society of Naval Architect and Marine Engineers) notations are used in the expression.

$$Y_A = Y_{\dot{u}}\dot{u} \qquad \& \qquad Y_{\dot{u}} = \frac{\partial Y}{\partial \dot{u}}$$

[36]

3.2.3.2 Coriolis and Centripetal Matrix

The coriolis and centripetal matrix also consists of two terms i.e rigid body and added mass terms. Mathematically it is given by

$$C(V) = C_{RB}(V) + C_A(V) \tag{3.24}$$

parametrization of C_{RB} is not unique. Using Newton Law's the Coriolis and centripetal matrix can be parameterized as

$$C_{RB} = \begin{bmatrix} 0_{3\times3} & -mS(v_1) - mS(v_2)\,S(r_G) \\ -mS(v_1) + mS(r_G)\,S(v_2) & -S(I_o v_2) \end{bmatrix} \tag{3.25}$$

C_{RB} is a skew-symmetric matrix i.e. $C_{RB} = -C_{RB}^T$

$$\begin{bmatrix} 0 & 0 & 0 & m(y_Gq+z_Gr) & -m(x_Gq-w) & -m(x_Gr+w) \\ 0 & 0 & 0 & -m(y_Gp+w) & m(z_Gr+x_Gp) & -m(y_Gr-u) \\ 0 & 0 & 0 & -m(z_Gp-v) & -m(z_Gq+u) & m(x_Gp+y_Gq) \\ -m(y_Gq+z_Gr) & m(x_Gq-w) & m(x_Gr+w) & 0 & -I_{yz}q-I_{xz}p+I_zr & -I_{yz}r+I_{xy}p+I_yq \\ m(y_Gp+w) & -m(z_Gr+x_Gp) & m(y_Gr-u) & I_{yz}q+I_{xz}p-I_zr & 0 & -I_{xz}r+I_{xy}q+I_xq \\ m(z_Gp-v) & m(z_Gq+u) & -m(x_Gp+y_Gq) & -I_{yz}r-I_{xy}p+I_yq & -I_{xz}r+I_{xy}q-I_xp & 0 \end{bmatrix} \tag{3.26}$$

Here m is the mass of the AUV, I is the inertia tensor and $r_G = \begin{bmatrix} x_G & y_G & z_G \end{bmatrix}$ is the position vector. The Coriolis and Centripetal matrix due to added mass is

given by

$$\begin{bmatrix} 0 & 0 & 0 & 0 & -a_3 & a_2 \\ 0 & 0 & 0 & a_3 & 0 & a_1 \\ 0 & 0 & 0 & -a_2 & a_1 & 0 \\ 0 & -a_3 & a_2 & 0 & -b_3 & b_2 \\ a_3 & 0 & -a_1 & b_3 & 0 & -b_1 \\ -a_2 & a_1 & 0 & -b_2 & b_1 & 0 \end{bmatrix} \tag{3.27}$$

where,

$$a_1 = X_{\dot{u}}u + X_{\dot{v}}v + X_{\dot{w}}w + X_{\dot{p}}p + X_{\dot{q}}q + X_{\dot{r}}r \tag{3.28}$$

$$a_2 = X_{\dot{v}}u + Y_{\dot{v}}v + Y_{\dot{w}}w + Y_{\dot{p}}p + Y_{\dot{q}}q + Y_{\dot{r}}r \tag{3.29}$$

$$a_3 = Z_{\dot{w}}u + Y_{\dot{w}}v + Z_{\dot{w}}w + Z_{\dot{p}}p + Z_{\dot{q}}q + Z_{\dot{r}}r \tag{3.30}$$

$$b_1 = X_{\dot{p}}u + Y_{\dot{p}}v + Z_{\dot{p}}w + K_{\dot{p}}p + K_{\dot{q}}q + K_{\dot{r}}r \tag{3.31}$$

$$b_2 = X_{\dot{q}}u + Y_{\dot{q}}v + Z_{\dot{q}}w + K_{\dot{q}}p + M_{\dot{q}}q + M_{\dot{r}}r \tag{3.32}$$

$$b_3 = X_{\dot{r}}u + Y_{\dot{r}}v + Z_{\dot{r}}w + K_{\dot{r}}p + M_{\dot{r}}q + N_{\dot{r}}r \tag{3.33}$$

3.2.3.3 Hydrodynamic Damping Matrix

The damping of underwater vehicle at high speed with 6 DOF is highly non-linear. By considering three planes of symmetry of vehicle and assuming that the AUV is moving with a slow speed results in only drag terms in the hydrodynamic damping matrix. The lift forces are negligible by taking the assumption of slow speed. we can separate the drag force into linear and quadratic terms $D(V) = D_q(V)+D_l(V)$. The linear term with the assumption of three planes of symmetry is given as:

$$D_l(V) = \begin{bmatrix} X_u & 0 & 0 & 0 & 0 & 0 \\ 0 & Y_v & 0 & 0 & 0 & 0 \\ 0 & 0 & Z_w & 0 & 0 & 0 \\ 0 & 0 & 0 & K_p & 0 & 0 \\ 0 & 0 & 0 & 0 & M_q & 0 \\ 0 & 0 & 0 & 0 & 0 & N_r \end{bmatrix} \tag{3.34}$$

The quadratic drag terms can be given by

$$D_q(V) = \begin{bmatrix} X_{u|u|}u & 0 & 0 & 0 & 0 & 0 \\ 0 & Y_{v|v|}v & 0 & 0 & 0 & 0 \\ 0 & 0 & Z_{w|w|}w & 0 & 0 & 0 \\ 0 & 0 & 0 & K_{p|p|}p & 0 & 0 \\ 0 & 0 & 0 & 0 & M_{q|q|}q & 0 \\ 0 & 0 & 0 & 0 & 0 & N_{r|r|}r \end{bmatrix} \tag{3.35}$$

where

$$X_{u|u|} = \partial X/\partial u|u| = -1/2\rho C_d A_f$$

C_d and A_f are reference drag and area co-efficient respectively.

3.2.3.4 Gravitational and Buoyancy Matrix

The gravitational and buoyancy Matrix consists of the forces on the AUV due to gravity and buoyancy

$$g(\eta) = \begin{bmatrix} (W-B)sin\theta \\ -(W-B)cos\theta sin\phi \\ -(W-B)cos\theta cos\phi \\ -(y_G W - y_B B)cos\theta cos\phi + (z_G W - z_B B)cos\theta sin\phi \\ (z_G W - z_B B)sin\theta + (x_G W - x_B B)cos\theta cos\phi \\ (x_G W - x_B B)cos\theta sin\phi + (y_G W - y_B B)sin\theta \end{bmatrix} \tag{3.36}$$

where $r_G = \begin{bmatrix} x_G & y_G & z_G \end{bmatrix}$ is the center of gravity and $r_B = \begin{bmatrix} x_B & y_B & z_B \end{bmatrix}$ is the center of buoyancy of the AUV respectively.

3.2.3.5 Thruster forces and moments

KAMBARA has 5 thrusters which enables it to move in 5 DOF surge, roll ,heave, yaw and pitch. The thruster forces and moment vector T is given by [10]

$$T = LU \tag{3.37}$$

where, U is the vector of thrust generated by 5 thruster

$$U = \begin{bmatrix} T1 \\ T2 \\ T3 \\ T4 \\ T5 \end{bmatrix} \tag{3.38}$$

and L is the mapping matrix given by

$$L = \begin{bmatrix} 1 & 1 & 0 & 0 & 0 \\ 0 & 0 & 0 & 0 & 0 \\ 0 & 0 & -1 & -1 & -1 \\ 0 & 0 & l_1 & -l_1 & 0 \\ -l_5 & -l_5 & l_3 & l_3 & -l_4 \\ l_2 & -l_2 & 0 & 0 & 0 \end{bmatrix} \tag{3.39}$$

Figure 3.5 shows the thrust diagram of KAMBARA. Where

T1= Thrust generated from left flat thruster

T2= Thrust generated from right flat thruster

T3= Thrust generated from left upright thruster

T4= Thrust generated from right front upright thruster

T5= Thrust generated from rear upright thruster

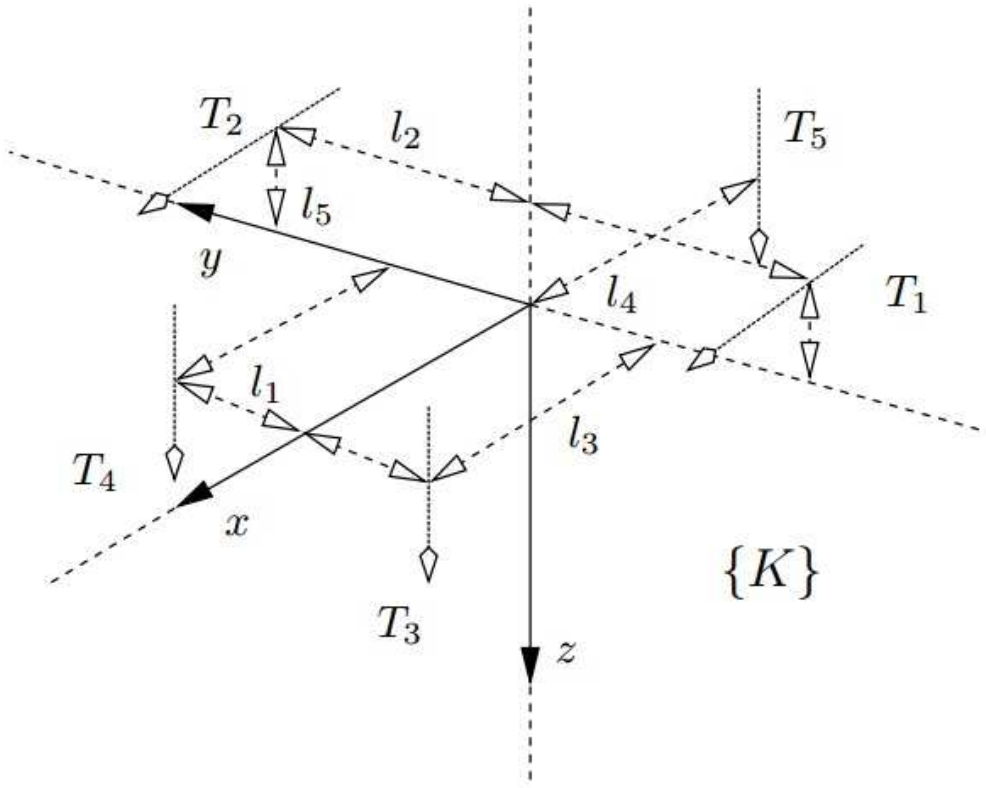

FIGURE 3.5: Thrust diagram in body frame involving parameters for the thrust mapping matrix L [10]

3.3 Ocean Currents

Ocean currents are circulating systems of ocean waters in horizontal and vertical directions . In the upper layer of the ocean the ocean currents main cause of generation is atmospheric winds. Ocean currents may also be caused by Coriolis effect, heat exchange (temperature of equator warmer than poles), salinity difference as well as density of the water [37] [9].

3.3.1 Ocean Currents in equation of motion

For simulation of AUVs it is quite important to include the environmental disturbances. For deeply submerged vessels we can neglect the wave-induced disturbance, so the only environmental disturbance to be tackled is ocean currents. We

can include the ocean currents in the dynamical equation of motion for AUV. Let,

$$V_c = [u_c^b, v_b^c, w_c^b, 0, 0, 0]^T \tag{3.40}$$

where, V_c is the body fixed current velocity, then

$$V_r = V - V_c \tag{3.41}$$

$$V_r = [u - u_c^b, v - v_b^c, w - w_c^b, p, q, r]^T \tag{3.42}$$

where,

u_c^b, v_b^c, w_c^b are the body fixed current velocities

It is commonly assumed that the current velocity V_c is varying slowly i.e $\dot{V}_c \approx 0$ such that $\dot{V}_r \approx 0$, then we can write the dynamical equation of motion as.

$$M\dot{V} + C\left(V_r\right)V_r + D\left(V_r\right)V_r + g\left(\eta\right) = \tau \tag{3.43}$$

Normally the current speed V_{cs} is defined in the ERF using flow axis that is $[V_{cs}, 0, 0]^T$ such that V_{cs} is directed along x. By defining flow angle of attack "(α_c) and flow sideslip angle (β_c) we can perform the transformation from flow axes to NED.

So by performing two principle rotations we can perform 3D-current velocities transformation [37] [38]

$$\begin{bmatrix} u_c^E \\ v_c^E \\ w_c^E \end{bmatrix} = C_{y,\alpha_c}^T C_{z,-\beta_c}^T \begin{bmatrix} V_{cs} \\ 0 \\ 0 \end{bmatrix} \tag{3.44}$$

here,

$C_{y,\alpha_c}, C_{z,-\beta_c}$ are rotation matrices defined as:

$$C_{y,\alpha_c} = \begin{bmatrix} cos\alpha_c & 0 & sin\alpha_c \\ 0 & 1 & 0 \\ -sin\alpha_c & 0 & cos\alpha_c \end{bmatrix} \tag{3.45}$$

$$C_{z,-\beta_c} = C_{z,\beta_c}^T = \begin{bmatrix} cos\beta_c & sin\beta_c & 0 \\ -sin\beta_c & cos\beta_c & 0 \\ 0 & 0 & 1 \end{bmatrix} \tag{3.46}$$

Using 3.44, 3.45, 3.46 we find out:

$$\begin{bmatrix} u_c^E \\ v_c^E \\ w_c^E \end{bmatrix} = \begin{bmatrix} V_{cs}cos\alpha_c cos\beta_c \\ V_{cs}sin\beta_c \\ V_{cs}cos\beta_c sin\alpha_c \end{bmatrix} \tag{3.47}$$

Then Euler angle of rotation can be used to transform the current velocities in ERF to body fixed velocities.

$$\begin{bmatrix} u_c^b \\ v_c^b \\ w_c^b \end{bmatrix} = J1^T(\eta_2) \begin{bmatrix} u_c^E \\ v_c^E \\ w_c^E \end{bmatrix} \tag{3.48}$$

for **2D case** $\alpha_c = 0$ then 3.47 reduces to

$$\begin{bmatrix} u_c^E \\ v_c^E \end{bmatrix} = \begin{bmatrix} V_{cs}cos\beta_c \\ V_{cs}sin\beta_c \end{bmatrix} \tag{3.49}$$

as the w_c^E component is not used in horizontal plane hence we can write by reducing 3.48

$$\begin{bmatrix} u_c^b \\ v_c^b \end{bmatrix} = \begin{bmatrix} V_{cs}cos(\beta_c - \psi) \\ V_{cs}sin(\beta_c - \psi) \end{bmatrix} \tag{3.50}$$

3.4 Open Loop Simulations

The parameters of KAMBARA AUV developed at the Robotic Systems Lab, The Australian National University, are used for open loop simulation .KAMBARA is a low cost AUV which has been designed as a platform for underwater robotics research. the length is 1.2m, width is 1.5m and height of 0.9m.
KAMBARA has five thrusters that are attached in two isolated planes. The structure allows a 5 DOF motion for KAMBARA: surge, heave, roll, pitch, and yaw. Sensors used in KAMBARA are [10]:

- compass
- inclinometer
- accelerometer
- rate gyro
- pressure sensor
- temperature sensor

The used parameters are:

FIGURE 3.6: Kambara Model [10]

3.4.1 Mass and Inertia Matrix

$$M_{RB} = \begin{bmatrix} 117 & 0 & 0 & 0 & 0 & 0 \\ 0 & 117 & 0 & 0 & 0 & 0 \\ 0 & 0 & 117 & 0 & 0 & 0 \\ 0 & 0 & 0 & 10.7 & 0 & 0 \\ 0 & 0 & 0 & 0 & 11.8 & 0 \\ 0 & 0 & 0 & 0 & 0 & 13.4 \end{bmatrix} \tag{3.51}$$

$$M_A = \begin{bmatrix} 58.4 & 0 & 0 & 0 & 0 & 0 \\ 0 & 23.8 & 0 & 0 & 0 & 0 \\ 0 & 0 & 117 & 0 & 0 & 0 \\ 0 & 0 & 0 & 10.7 & 0 & 0 \\ 0 & 0 & 0 & 0 & 11.8 & 0 \\ 0 & 0 & 0 & 0 & 0 & 13.4 \end{bmatrix} \tag{3.52}$$

3.4.2 Coriolis and Centripetal Matrix

$$C_{RB} = \begin{bmatrix} 0 & 0 & 0 & 0 & 117w & -117v \\ 0 & 0 & 0 & -117w & 0 & 117u \\ 0 & 0 & 0 & 117v & -117u & 0 \\ 0 & 117w & -117v & 0 & 13.4r & -11.8q \\ -117w & 0 & 117u & -13.4r & 0 & 10.7p \\ 117v & -117u & 0 & 11.8q & -10.7p & 0 \end{bmatrix} \tag{3.53}$$

$$C_A = \begin{bmatrix} 0 & 0 & 0 & 0 & 23.8w & -23.8v \\ 0 & 0 & 0 & -23.8w & 0 & 58.4u \\ 0 & 0 & 0 & 23.8v & -58.4u & 0 \\ 0 & 23.8w & -23.8v & 0 & 2.67r & -1.18q \\ -23.8w & 0 & 58.4u & -2.67r & 0 & 3.38p \\ 23.8v & -58.4u & 0 & 1.18q & -3.38p & 0 \end{bmatrix} \tag{3.54}$$

3.4.3 Hydrodynamic Damping Matrix

$$\begin{bmatrix} D = 120 + 90|u| & 0 & 0 & 0 & 0 & 0 \\ 0 & 90 + 90|v| & 0 & 0 & 0 & 0 \\ 0 & 0 & 150 + 90|w| & 0 & 0 & 0 \\ 0 & 0 & 0 & 15 + 10|p| & 0 & 0 \\ 0 & 0 & 0 & -0 & 15 + 12|q| & 0 \\ 0 & 0 & 0 & 0 & 0 & 18 + 15|r| \end{bmatrix} \tag{3.55}$$

The matrix consists of linear and quadratic drag force terms.

3.4.4 Gravitational and Buoyancy Forces Vector

By taking $r_G = \begin{bmatrix} 0 & 0 & 0 \end{bmatrix}, r_B = \begin{bmatrix} -0.017 & 0 & -0.115 \end{bmatrix}$, B=1108N, W=1148N, here we get $BG = \begin{bmatrix} 0.017 & 0 & 0.115 \end{bmatrix}$. BG is the distance between center of origin and center of buoyancy. The matrix used is 3.36

3.4.5 Thrust Mapping Matrix

$$L = \begin{bmatrix} 1 & 1 & 0 & 0 & 0 \\ 0 & 0 & 0 & 0 & 0 \\ 1 & 1 & -1 & -1 & -1 \\ 0 & 0 & -0.28 & 0.28 & 0 \\ 0.05 & 0.05 & -0.32 & -0.32 & 0.43 \\ 0.47 & -0.47 & 0 & 0 & 0 \end{bmatrix} \tag{3.56}$$

Case 01

The buoyancy vector taken is as , $r_B = \begin{bmatrix} -0.017 & 0 & -0.115 \end{bmatrix}$, and buoyancy force less than gravitational force , i.e, B=1108N and W= 1170 N.

With all initial conditions setting to 0 and no input applied the simulations results are shown. Figure 3.7 represents the translational motion of the KAMBARA which shows the vehicle is submerging and moving along the x-axis, the reason is as we have taken weight greater than the buoyancy force and buoyancy is not aligned with center of gravity which results in a moment. Figure 3.8 represents the orientation of the vehicle showing pitching of the AUV. Figure 3.9 and Figure 3.10 shows the linear and angular velocities for KAMBARA.

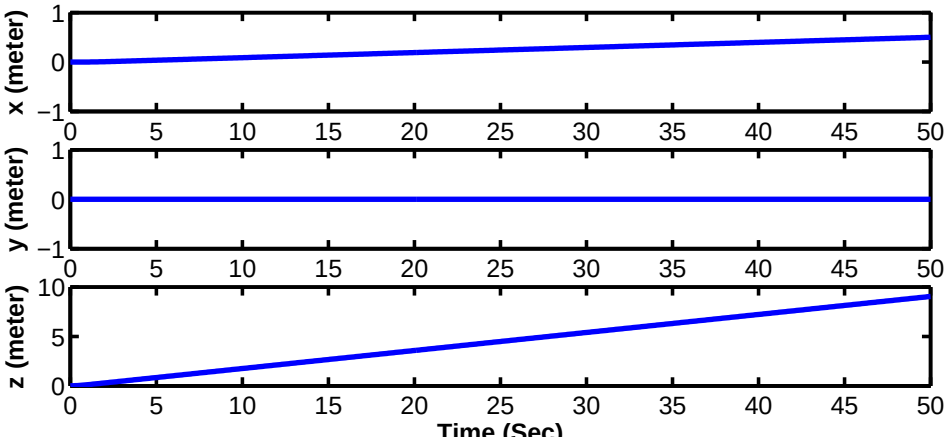

FIGURE 3.7: Position of KAMBARA

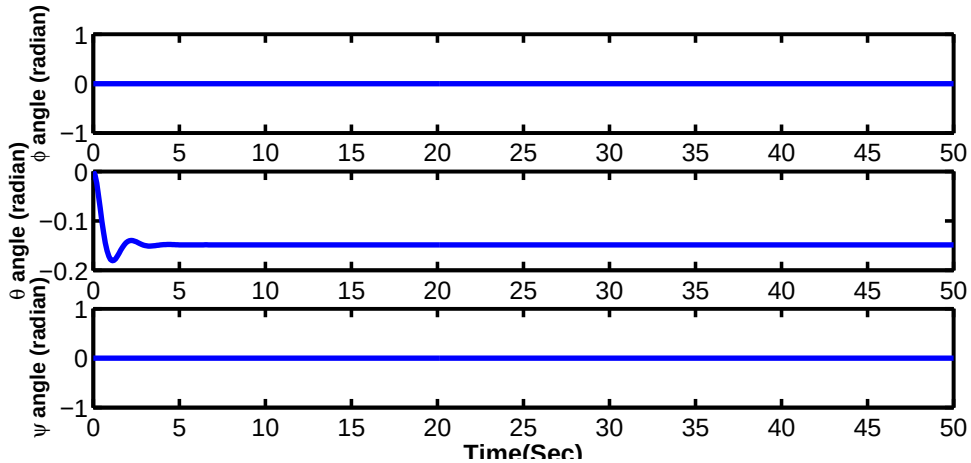

FIGURE 3.8: Orientation of KAMBARA

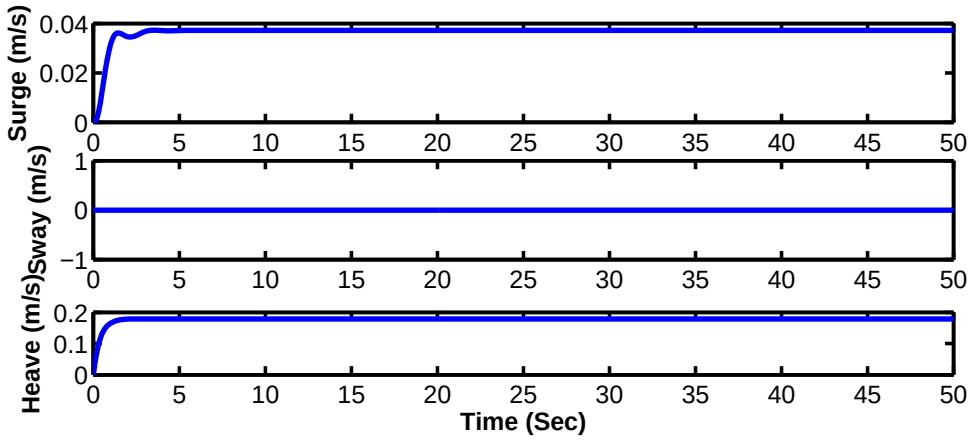

FIGURE 3.9: linear velocities of KAMBARA

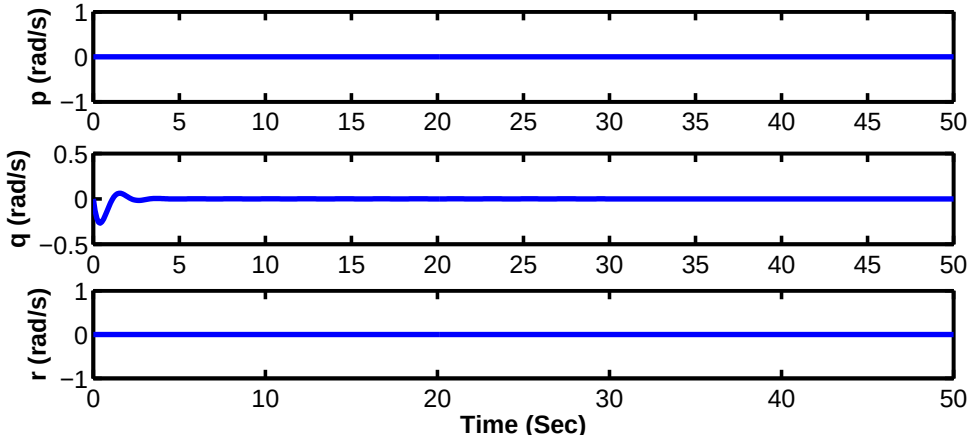

FIGURE 3.10: Angular velocities of KAMBARA

CASE 02

Taking buoyancy vector as $r_B = \begin{bmatrix} -0.017 & 0 & -0.115 \end{bmatrix}$ and buoyancy force less than gravitational force i.e, B=1108N and W= 1170 N.

With all initial conditions setting to 0 and applying maximum input in surge direction.

- Omega1 (propeller speed for motor 1)= 200 rpm
- Omega2 (propeller speed for motor 2)= 200 rpm

The simulations results are shown where Figure 3.11, Figure 3.12, Figure 3.13, Figure 3.14 shows translation, orientation, linear velocities and angular velocities of KAMBARA. Due to the propellers thrust along the surge direction we see in Figure 3.13 that the surge velocity has increased to approx 0.7m/s. The results show us that the KAMBARA can approach to a velocity of approx 0.7 m/s when maximum input is applied to it.

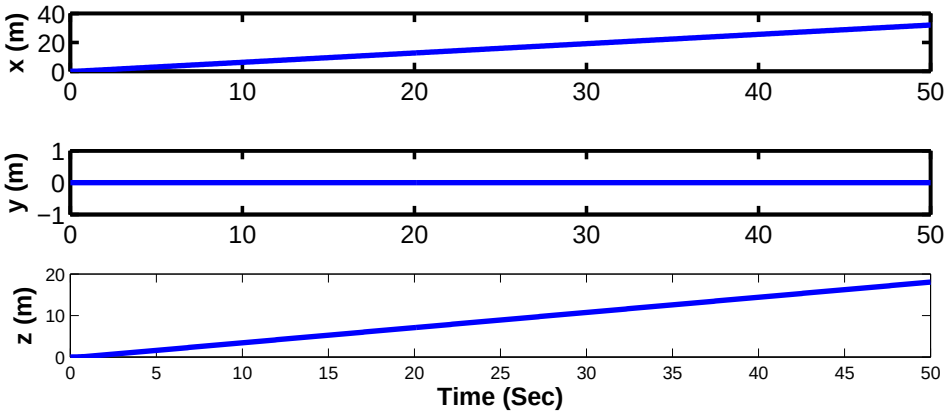

FIGURE 3.11: Position of KAMBARA

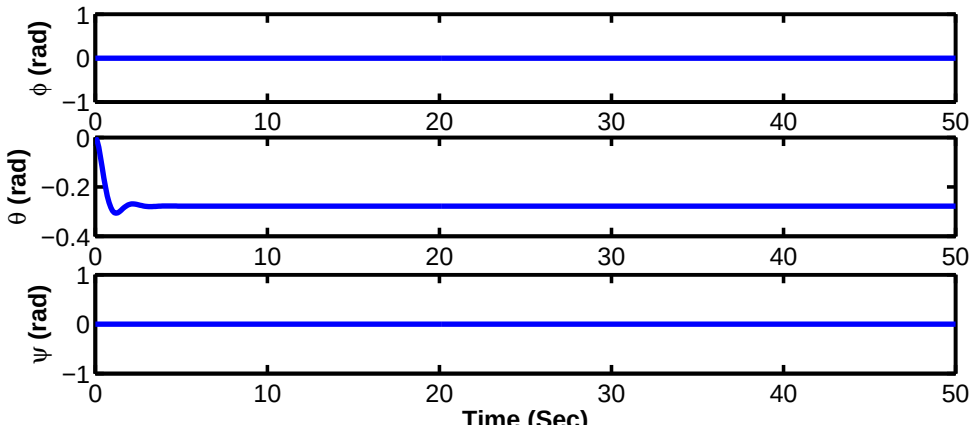

FIGURE 3.12: Orientation of KAMBARA

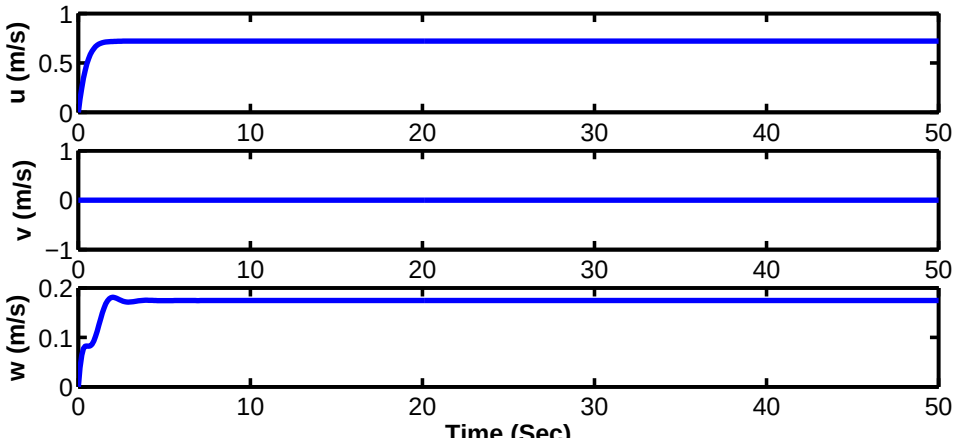

FIGURE 3.13: Linear velocities of KAMBARA

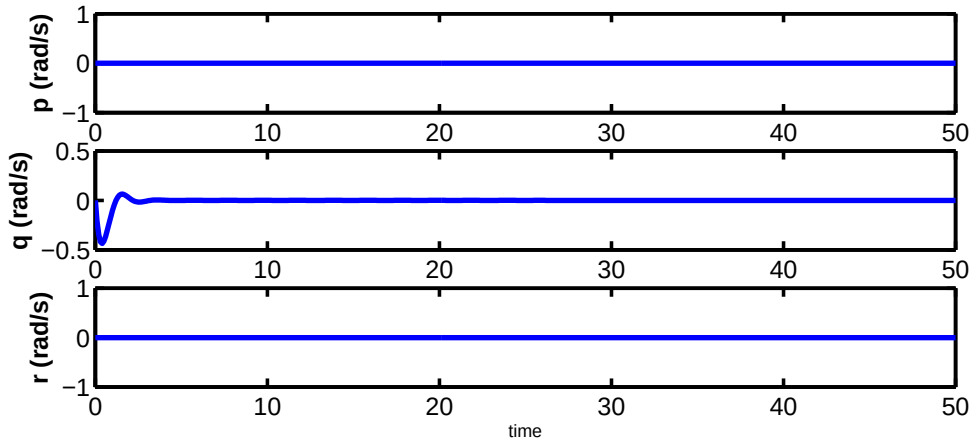

FIGURE 3.14: angular velocities of KAMBARA

The Open loop results of the vehicle depicts that KAMBARA always has a pitch angle -0.269 radians (-15.412565 degree) due to the misalignment of the COB and COG. It further explains that the vehicle will submerge if kept in water due to the reason $W > B$.

Chapter 4

CONTROLLER DESIGN FOR KAMBARA AUV

KAMBARA is a slow moving AUV that can move in 5 DOF resulting in an under-actuated under water vehicle. It can move in surge, heave, roll, pitch and yaw direction while no direct input is provided for movement in sway direction. The thrusters of KAMBARA are highly coupled in the 5 DOF motion due to its configuration. As a results a single thruster is not enough to move the vehicle in one direction rather combinations of two or more thrusters is used to achieve the required DOF motion.

This chapter covers the details of the controller design for KAMBARA AUV. A PID controller is designed for the vehicle followed by a sliding mode controller and accuracy of both the controllers is compared. The chapter also includes results of both controllers in the presence of ocean currents (model discussed in chapter 03)

4.1 PID Control for KAMBARA

Authors have proposed PID controllers in the literature, [13] uses PID control for steering, diving and speed of AUV. PID control is used for heading and depth of Mana-type unmanned underwater test vehicle in [14] i.e. only 2 DOF. The study here covers the design of PID controller for the 5 DOF motion of KAMBARA.

Pitch, heading, roll, depth and translation in x of the vehicle are controlled using PID control technique. All the controllers are implemented in MATLAB-SIMULINK using S-function. Maximum rpm that can be generated by the single

thruster is 1909 rpm, the corresponding rpm generated for the controlled task is shown to be within the limits of all the five thrusters. Figure 4.1 shows the approach used to design the control of the required state. State required to control is feedback which gives the error, PID gives the required rpm of the motors for the control task, This rpm is transformed to the thrust from 5 thrusters using the relation 4.1.

$$U = K_{thr}\Omega|\Omega| \tag{4.1}$$

Where,

Ω is the motor shaft angular velocity and K_{thr} is a constant thrust value . The thrust vector of the motors (5×1) is mapped to mathematical model using the relation 3.37

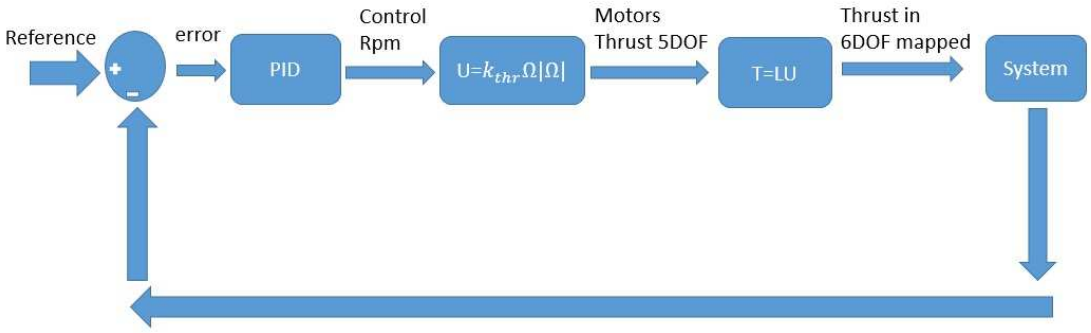

FIGURE 4.1: General Block diagram for PID control

The gains k_p, k_D, K_i for PID were selected by hit and trial method. The gains which gave the best results in terms of rise time, settling time and overshoot were selected for the control task.

4.1.1 Depth control with PID

Depth control using PID calculates thrust needed to achieve the desired depth. The vehicle was provided with a desired depth of 5m (z-positive downwards) by

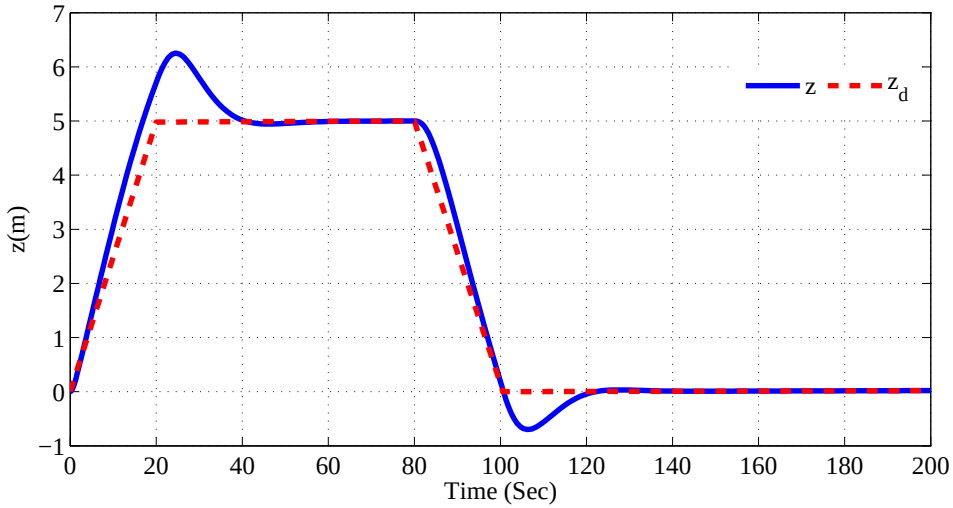

FIGURE 4.2: Depth control of KAMBARA with PID

selecting the gains k_p, k_d, k_i appropriately and then brought back to its initial position. The results also shows that the heave velocity is not exceeded from the maximum saturation limit of the vehicle, as shown Figure 4.3.

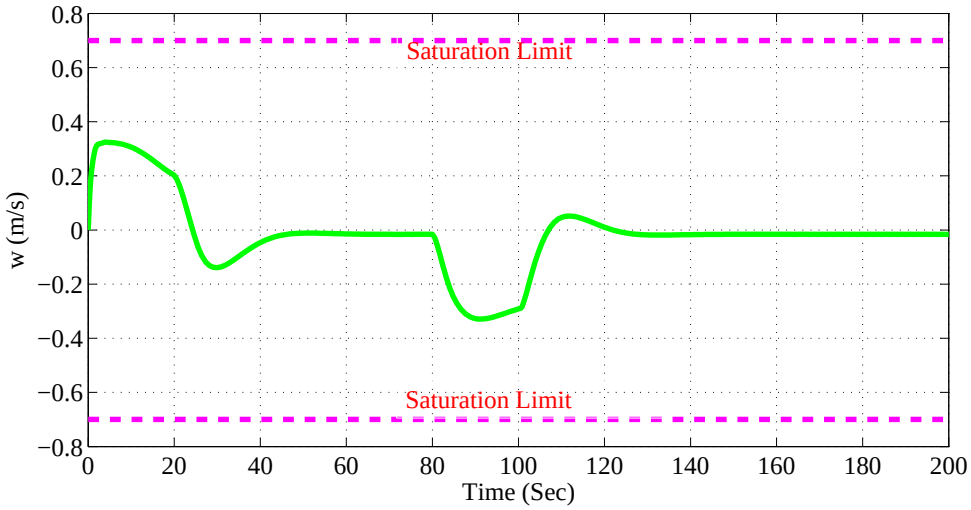

FIGURE 4.3: Heave velocity of KAMBARA as a result of depth control (PID)

4.1.2 Roll Control

The desired roll provided to KAMBARA was 0.35 rad ($\approx$ 20 deg). The simulation results shows that it takes about 50 sec for the vehicle to achieve the desired angle.

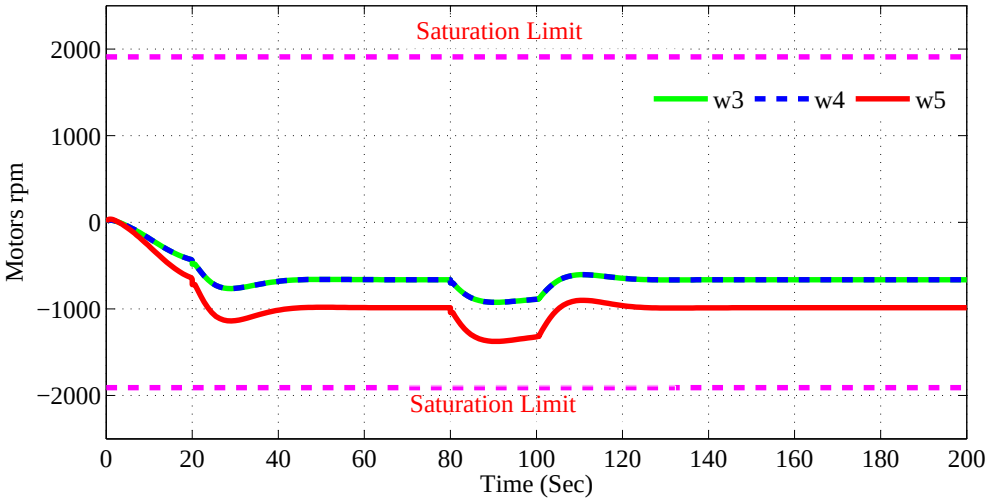

FIGURE 4.4: Control input for depth control of KAMBARA using PID

The zoomed portion shows the accuracy of the designed PID controller, while the control rpm generated is also within the saturation limits as shown in Figure 4.6

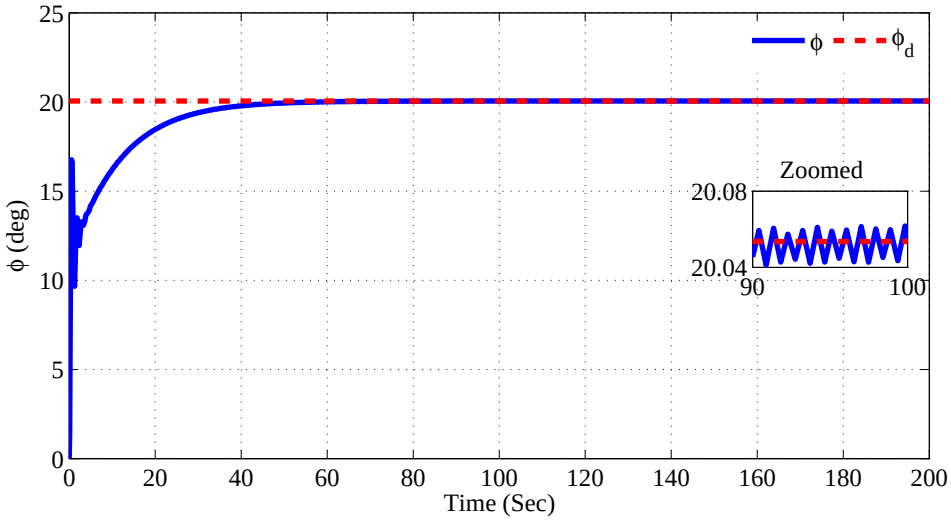

FIGURE 4.5: Roll control of KAMBARA with PID

4.1.3 Heading Control

Heading control was achieved using PID by giving the desired yaw of 0.35 radian ($\approx$ 20 degree). The desired ψ is achieved in about 15 sec with control input within

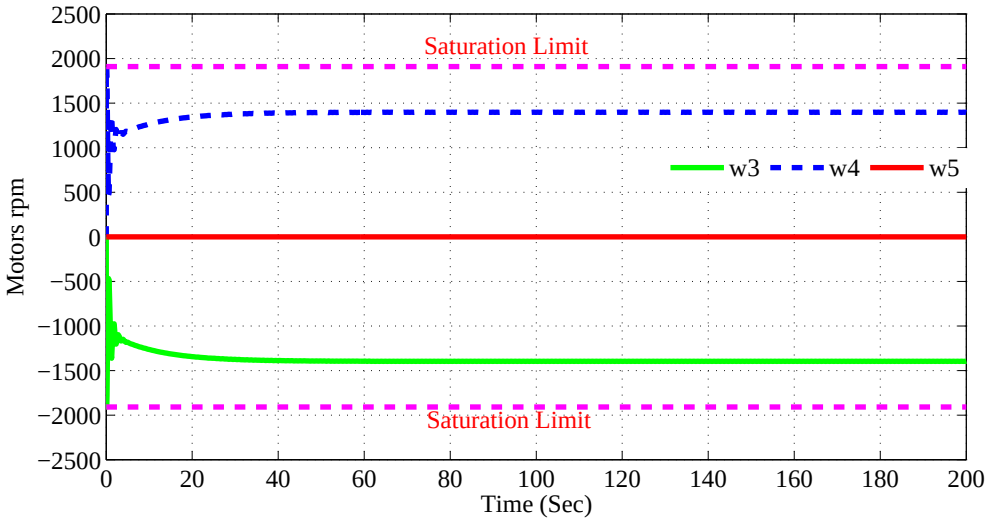

FIGURE 4.6: Control input for roll control of KAMBARA using PID

the maximum saturation limit. The results are shown in Figure 4.7 and Figure 4.8

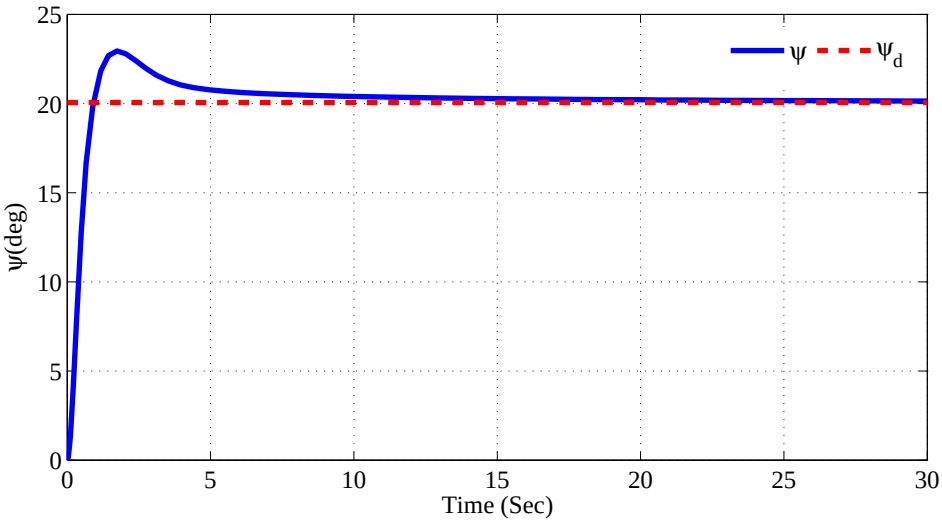

FIGURE 4.7: Heading control of KAMBARA with PID

4.1.4 Pitch Control

The desired pitch was achieved by selecting the gains of PID appropriately. PID control gives the required thrust to achieve the reference angle of 0.35 radians in

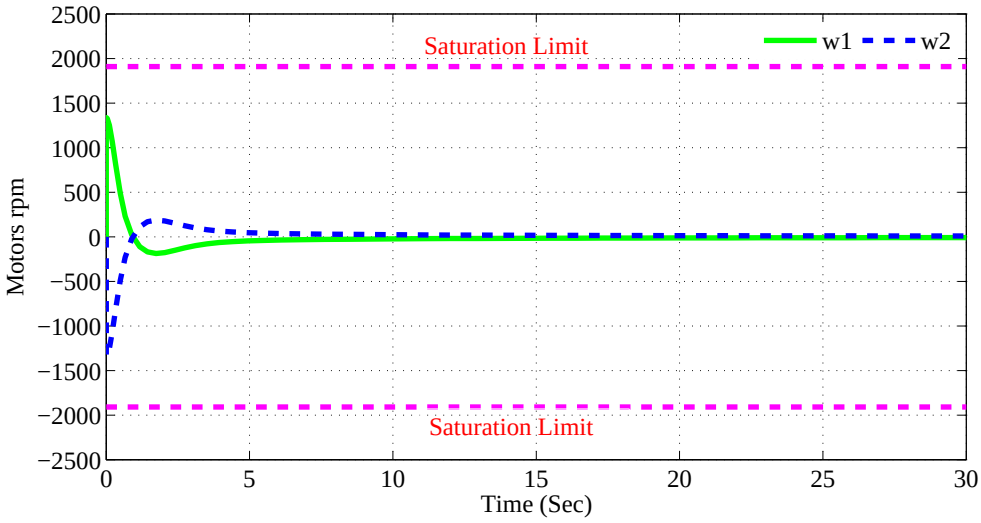

FIGURE 4.8: Control input for yaw control of KAMBARA using PID

about 30 seconds. Figure 4.9 and Figure 4.10 shows the simulation results of the controller.

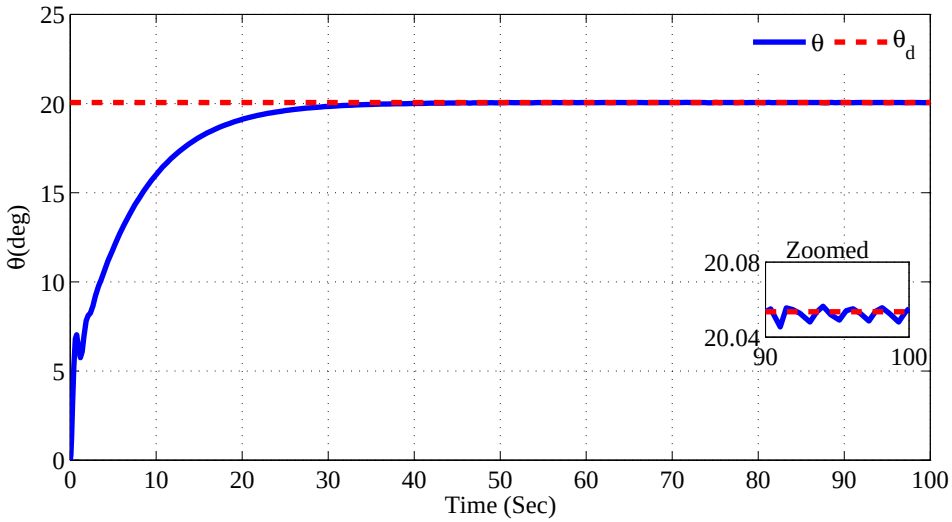

FIGURE 4.9: Pitch control of KAMBARA with PID

4.1.5 Combined controller

Pitch, roll, psi and depth controllers are combined together with the main idea to move the AUV down under water and again back towards its initial position

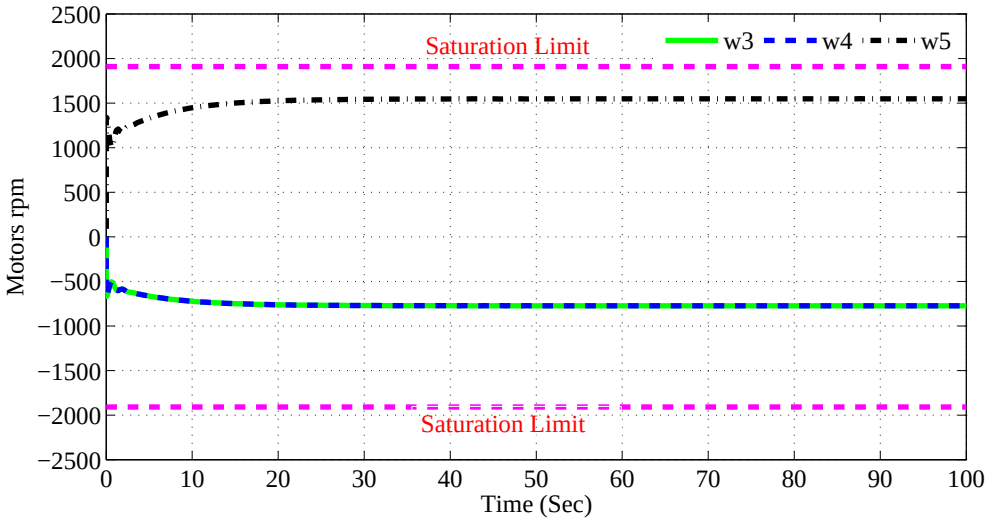

FIGURE 4.10: Control input for pitch control of KAMBARA using PID

without producing roll and pitch angle. The yaw angle is desired to be 0.5 rad ($\approx 28.6^o$). Initial condition was set to 10 degree for roll, pitch and psi. The simulation result in Figure 4.11 shows the settling time for ϕ angle is about 3 sec while for θ is about 13 sec. The ψ_d is has a settling time of approx 20 sec, while the desired depth is achieved with some overshoot as shown in the zoomed portion Figure 4.12. It is also shown in Figure 4.13 that the heave velocity is within the maximum vehicle limit, the Figure 4.14 shows that the motors rpm is not exceeded the saturation limit.

4.1.6 Closed-loop reference in xz-plane

To check the performance of designed controller a closed-loop reference was provided to the vehicle. The vehicle was desired to move from initial position to a depth of 2.5 m, it was then to move forward in x-direction to a 3m distance, was brought back to surface and finally moved back to initial starting point. The simulation results are shown below. It can be seen in Figure 4.15 and Figure 4.16 that the vehicle followed the desired path in accurate way and the thrusters rpm required to achieve this closed-loop reference were well within the limits.

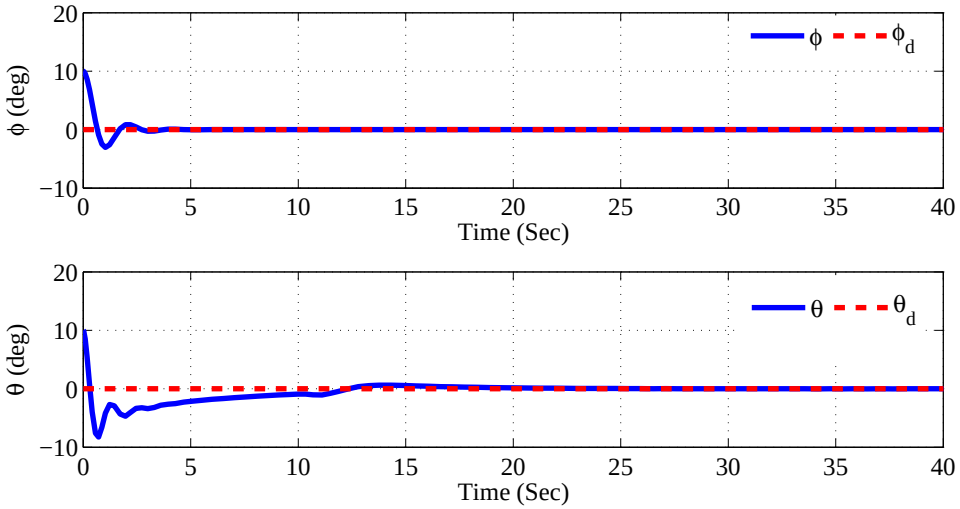

FIGURE 4.11: Control results of ϕ, θ

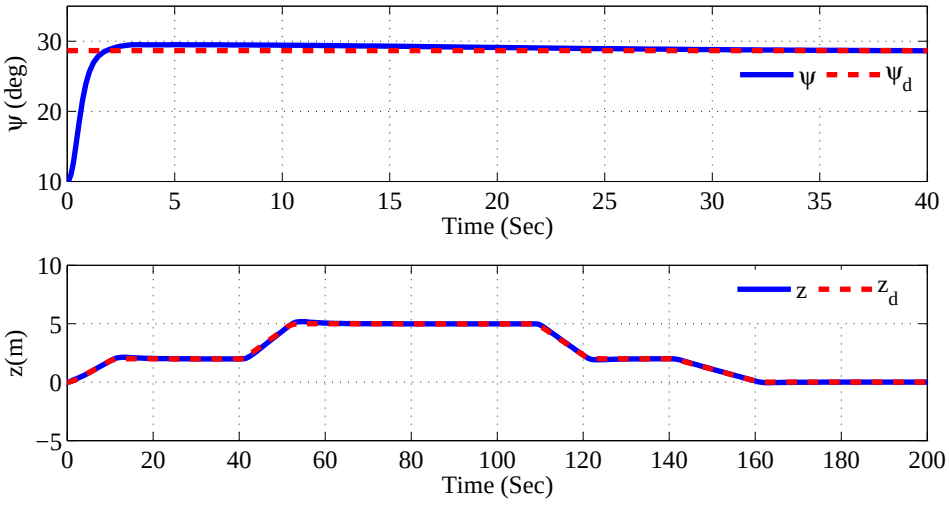

FIGURE 4.12: Control results of ψ, z

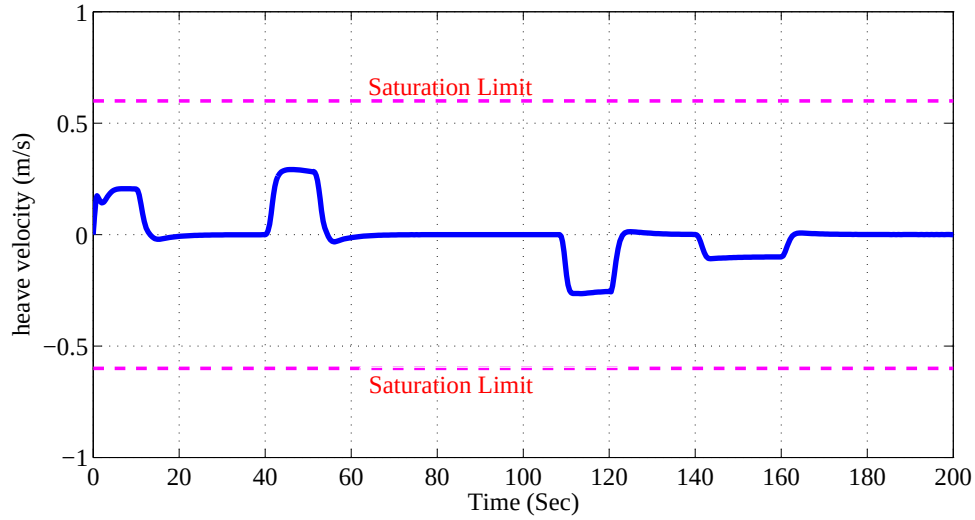

FIGURE 4.13: Heave velocity

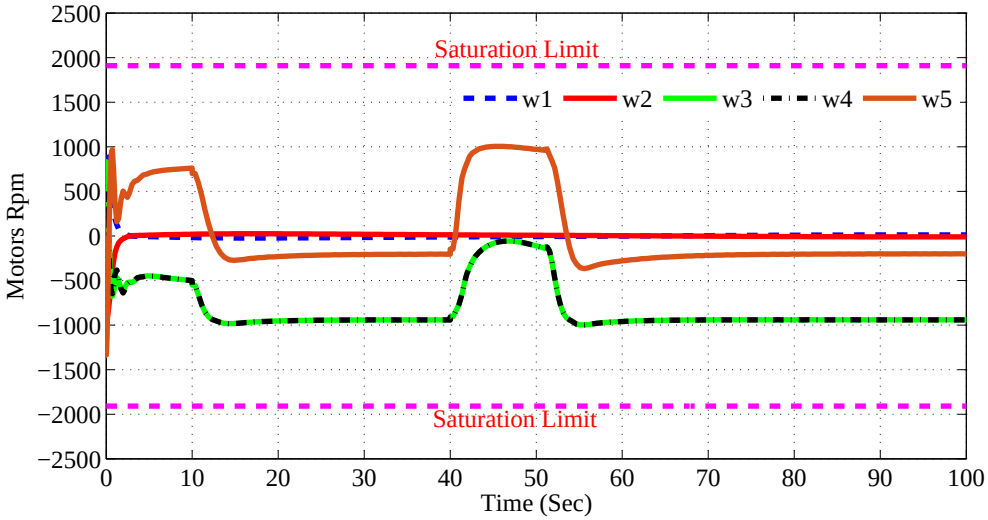

FIGURE 4.14: Control input for combined states control of KAMBARA using PID

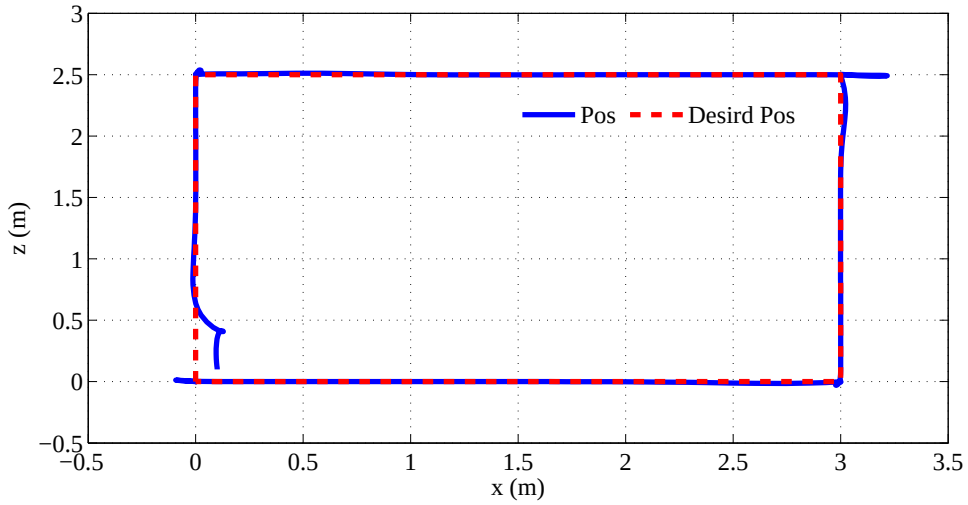

FIGURE 4.15: Closed-loop mission in xz-plane

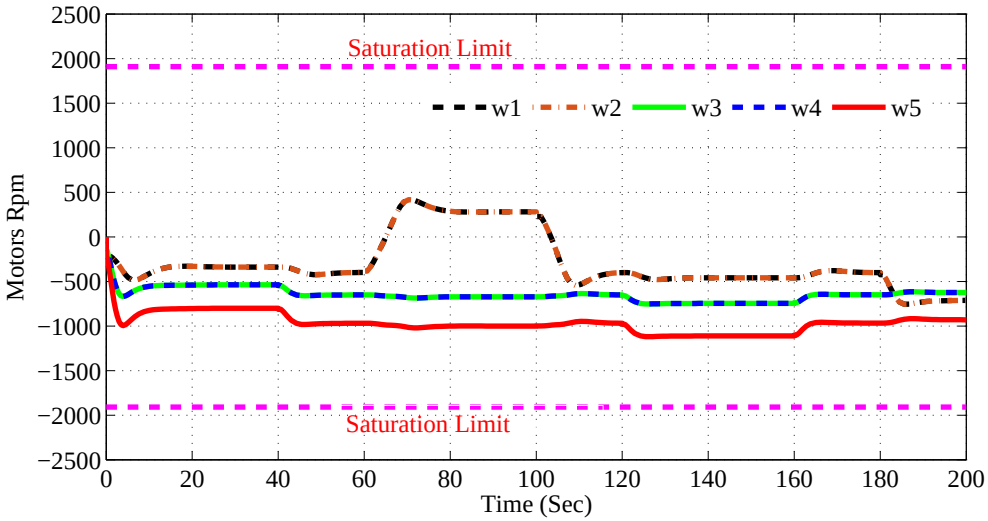

FIGURE 4.16: Control input for closed-loop trajectory of KAMBARA using PID

4.2 Sliding Mode Control

The basic concept of Sliding Mode Control (SMC) is to enforce sliding modes in a pre-defined manifold called the sliding surface/ sliding manifold/ switching line or hyper plane in a given system state space with the application of discontinuous (switching) controller.
SMC occurs in two phases

1. Reaching phase

   The phase in which system states trajectories are forced from initial condition to a pre-defined sliding surface by discontinuous controller.

2. Sliding phase

   This phase restricts the state trajectories on the sliding surface and are allowed to slide along the surface to an equilibrium (usually origin).

Sliding mode control provides guaranteed robustness against model imperfections, parametric uncertainties , parametric variations and external disturbances (usually matched and bounded). These properties of SMC proves to provide an accurate controller for KAMBARA in the presence of model uncertainties and disturbances.

4.2.1 Tracking with Sliding Mode control

In order to achieve the tracking of desired state, error 'e' is defined as

$$e = \eta_d - \eta \tag{4.2}$$

$$\dot{e} = -\dot{\eta} \tag{4.3}$$

$$\ddot{e} = -\ddot{\eta} \tag{4.4}$$

where η_d is desired state vector and η is the current state vector defined in 3.1.

The equation 3.20 can be written as

$$M\ddot{\eta} + C\left(\dot{\eta}\right)\dot{\eta} + D\left(\dot{\eta}\right)\dot{\eta} + g\left(\eta\right) = \tau \tag{4.5}$$

substituting equations 4.2, 4.3, 4.4 in equation 4.5, we get the relation given by

$$\ddot{e} = M^{-1}\left(-C\left(-\dot{e}\right)\dot{e} - D\left(-\dot{e}\right)\dot{e} + g\left(-\dot{e}\right) - T\right) \tag{4.6}$$

Defining sliding surface [39]

$$S = \Lambda e + \dot{e} \tag{4.7}$$

$$\dot{S} = \Lambda\dot{e} + \ddot{e} \tag{4.8}$$

Taking the Lyponove function candidate [39] [40]

$$V = \frac{1}{2}S^T M S \tag{4.9}$$

$$\dot{V} = S^T M\dot{S} + \frac{1}{2}S^T\dot{M}S \tag{4.10}$$

$$\dot{V} = S^T(M\Lambda\dot{e} + \frac{1}{2}(\dot{M} - 2C)S - D\dot{e} + g - \tau + C\Lambda e) \tag{4.11}$$

using the skew symmetry property of $(\dot{M} - 2C)$ matrix we get

$$\dot{V} = S^T(M\Lambda\dot{e} - D\dot{e} + g - \tau + C\Lambda e) \tag{4.12}$$

Using the relation 3.37 we can deduce the control law as

$$U = L^{-1}(M\Lambda\dot{e} - D\dot{e} + g + C\Lambda e + K sat(S)) \tag{4.13}$$

where K is a 6×6 diagonal gain matrix, and $sat\,(S)$ is a saturation function that provides a very smooth, chatter free control function.

4.2.2 Depth Control

Using the control law derived in 4.13 and providing the desired reference of 5m downwards, the designed sliding mode control gives a quite accurate tracking of the desired depth with no overshoot as can be seen in Figure 4.17. The Figure also shows the heave velocity to be within the maximum limit that can be achieved by KAMBARA. Figure 4.18 shows the motors/thrusters rpm to be in the limit and the sliding surface goes to zero, which shows that reaching phase has been achieved and the system is in the sliding phase.

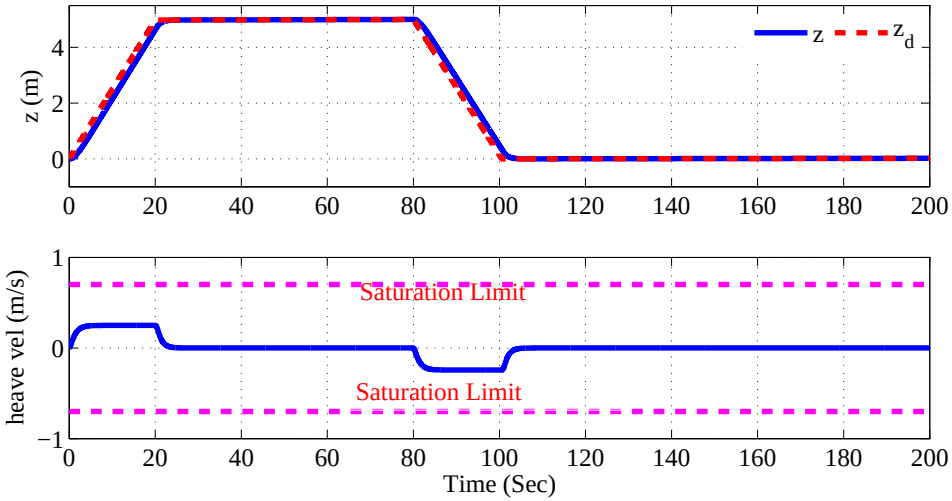

FIGURE 4.17: Depth and Heave velocity of KAMBARA

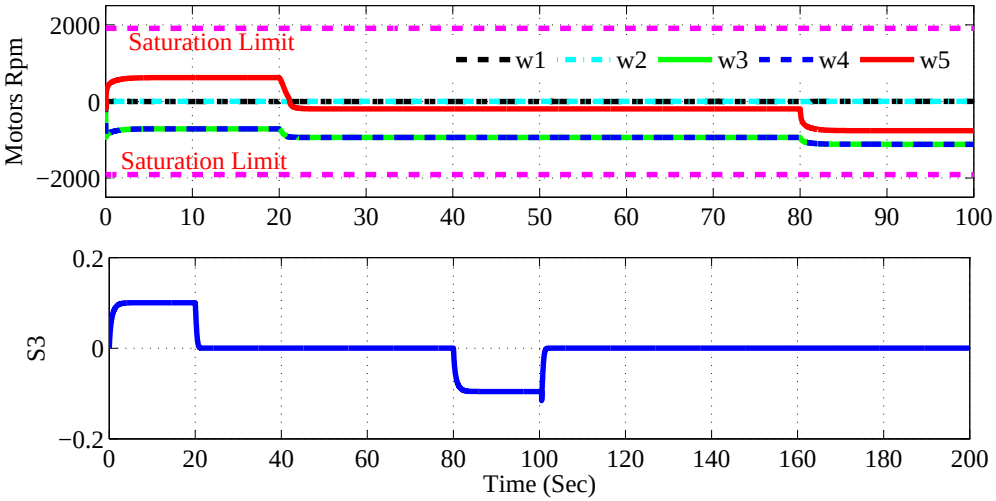

FIGURE 4.18: Motors rpm and sliding surface

4.2.3 Roll Control

For roll control of KAMBARA a reference of 0.35 rad was provided and adjusting the controller gain Figure 4.19 shows the result of the designed controller, we can see that the SMC achieve the desired reference quite smoothly and efficiently with the rpm of motors within the maximum saturation limit, Figure 4.20.

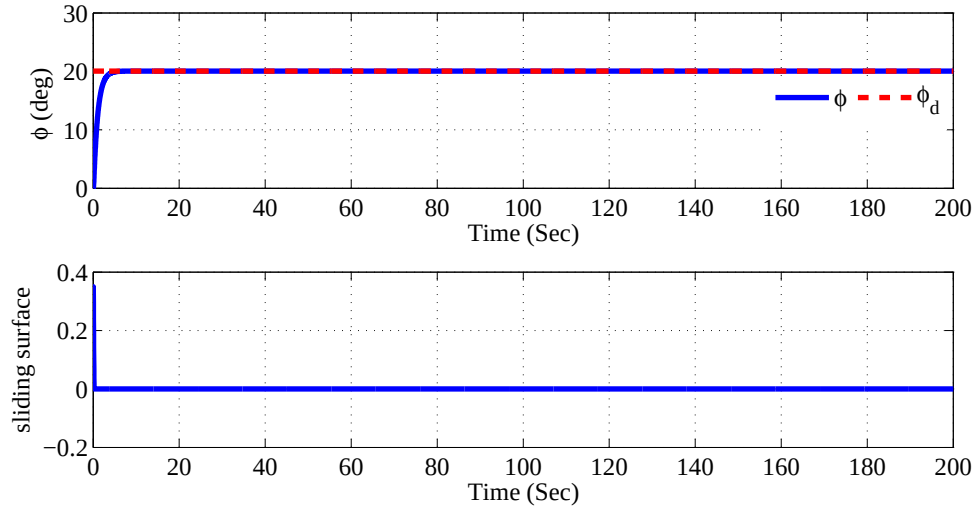

FIGURE 4.19: Roll control of KAMBARA with SMC and sliding surface for roll

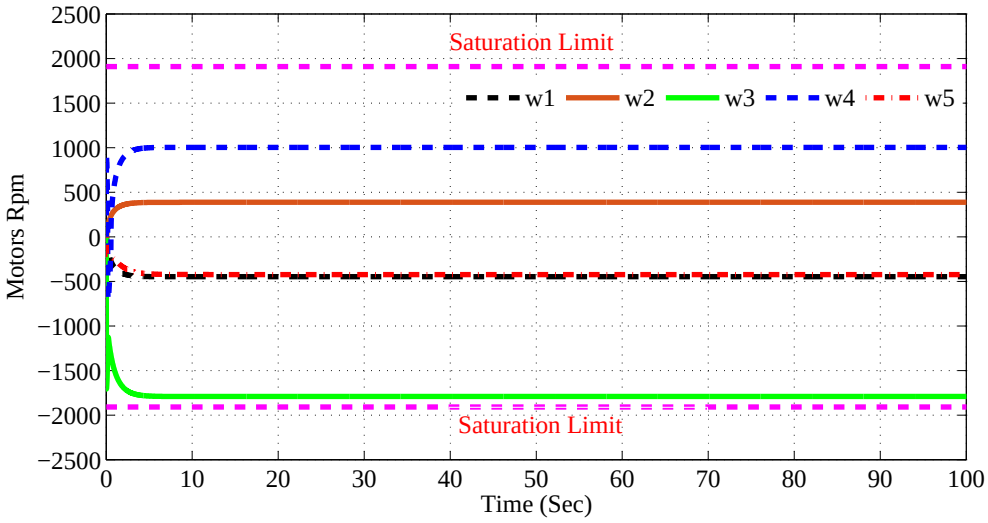

FIGURE 4.20: Motors rpm generated by SMC for roll control

4.2.4 Heading Control

The designed controller was used to achieve the desired yaw angle of 0.35 radian. The results achieved are shown in Figure 4.21, Figure 4.22. The sliding surface is shown to be going to zero depicting the completion of reaching phase and the input from motors is also shown to be within the desired limits.

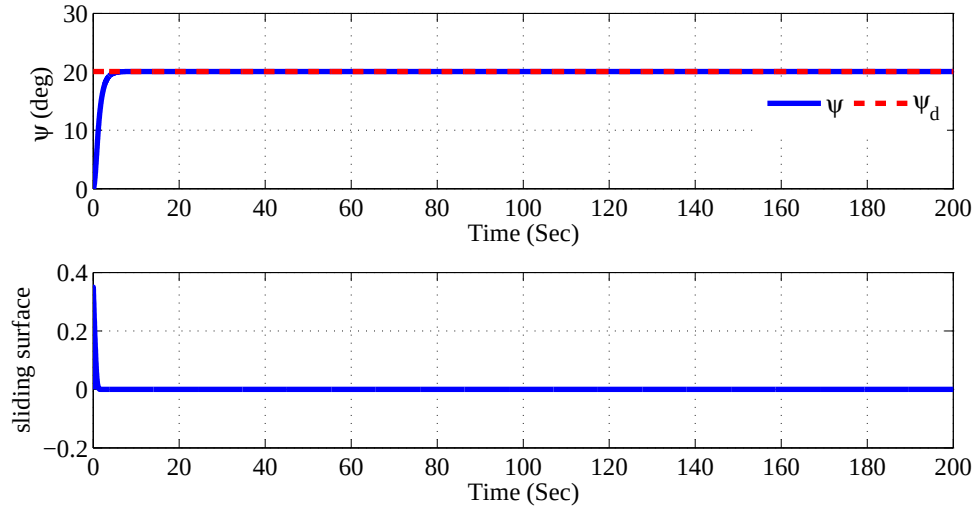

FIGURE 4.21: Heading control of KAMBARA with SMC and sliding surface for heading

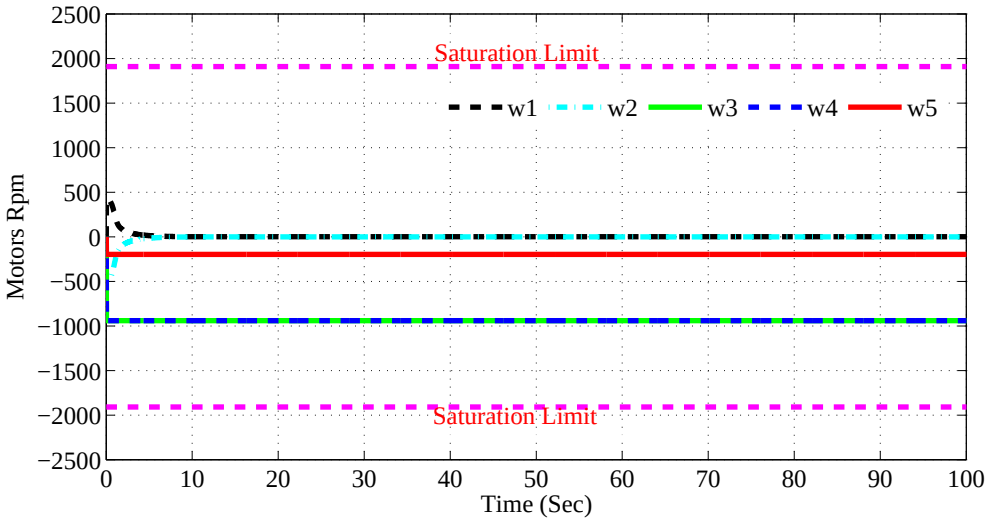

FIGURE 4.22: Motors rpm generated by SMC for heading control

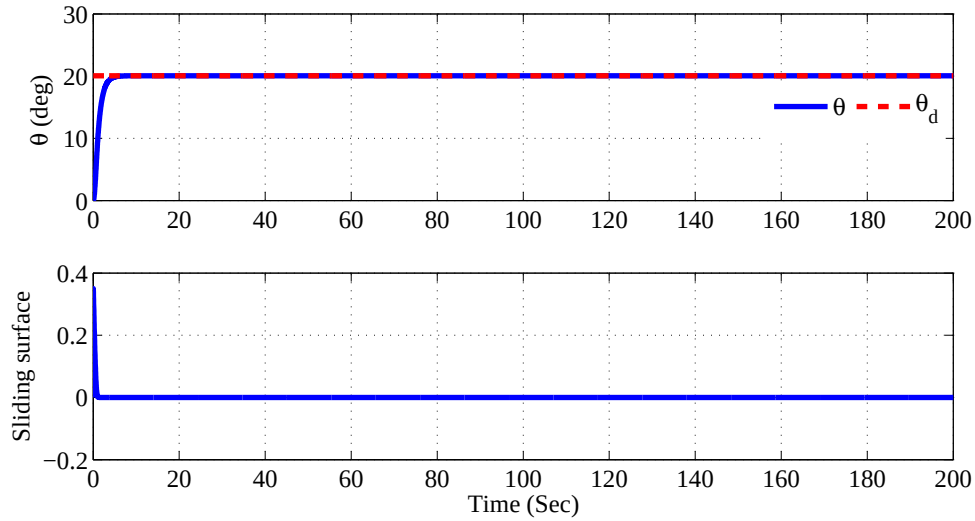

FIGURE 4.23: Pitch control of KAMBARA with SMC and sliding surface for pitch

4.2.5 Pitch Control

For the pitch control KAMABARA was given a desired depth of 0.35 radian (Figure 4.23) which is achieved with sliding mode control with no overshoot and settling time of about 5 seconds. The controlled input from the motors is shown in Figure 4.24 to be within desired limit.

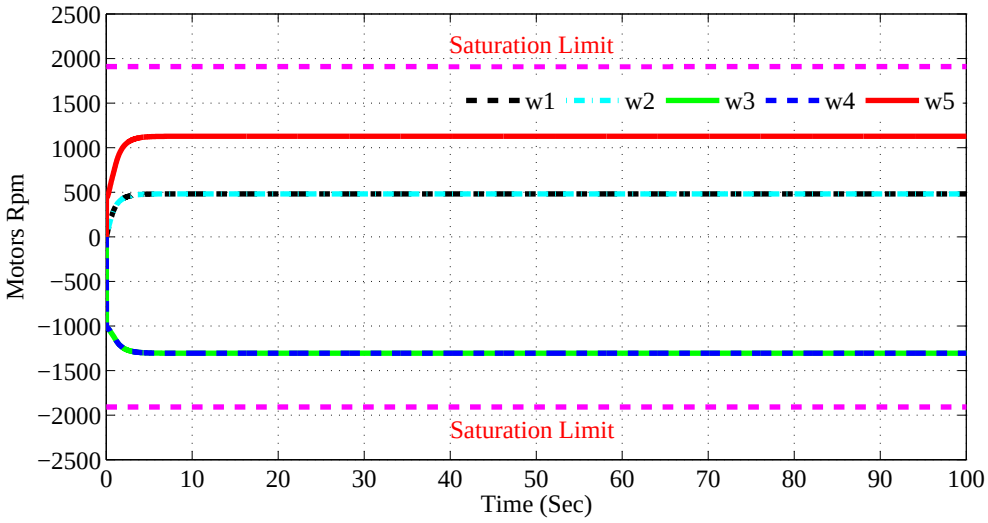

FIGURE 4.24: Motors rpm generated by SMC for pitch control

4.2.6 Combined Control

The same idea was used as in section (4.1.5). Initial condition for ϕ, θ and ψ was set to 10 degree. The AUV was desired to move underwater to a distance of 5m with with desired roll of zero degree. The AUV was provided with a desired angle of 0.26 radian ($\approx 15deg$) in pitch and psi DOF. The results obtained are shown in Figure 4.25- Figure 4.29. All the desired sliding surfaces are shown to be going to zero and the desired states are achieved accurately, while the controlled input was within the maximum saturation limit.

4.2.7 Closed-loop reference in xz-plane

KAMBARA was provided a closed-loop reference in xz-plane to check the performance of the designed sliding mode controller. The vehicle was desired to achieve a depth of 2.5 meter, translation in x of 3m and then brought back to its initial position of x= 0, z= 0. At start the vehicle initial state was kept at x= 0.2m and z= 0.2m. Results are shown in Figure 4.30, Figure 4.31, Figure 4.32.

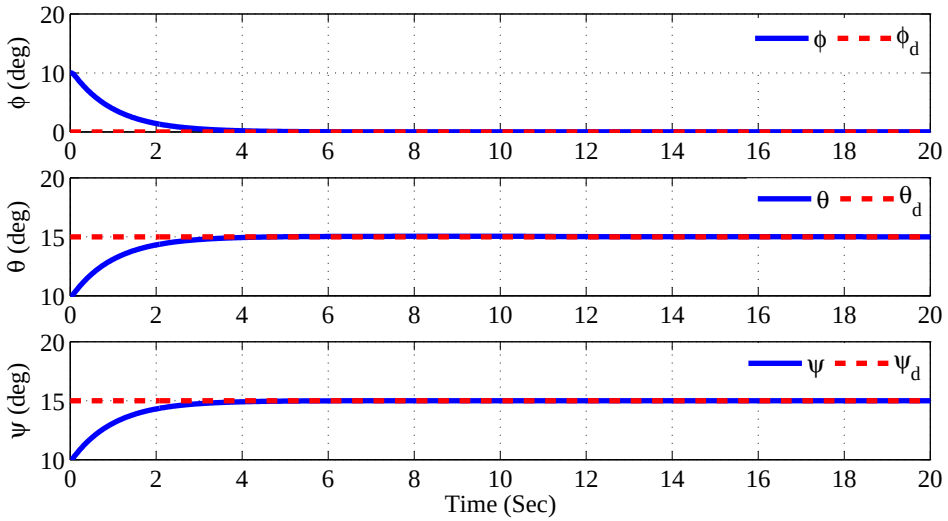

FIGURE 4.25: Roll, Pitch and Psi control with SMC

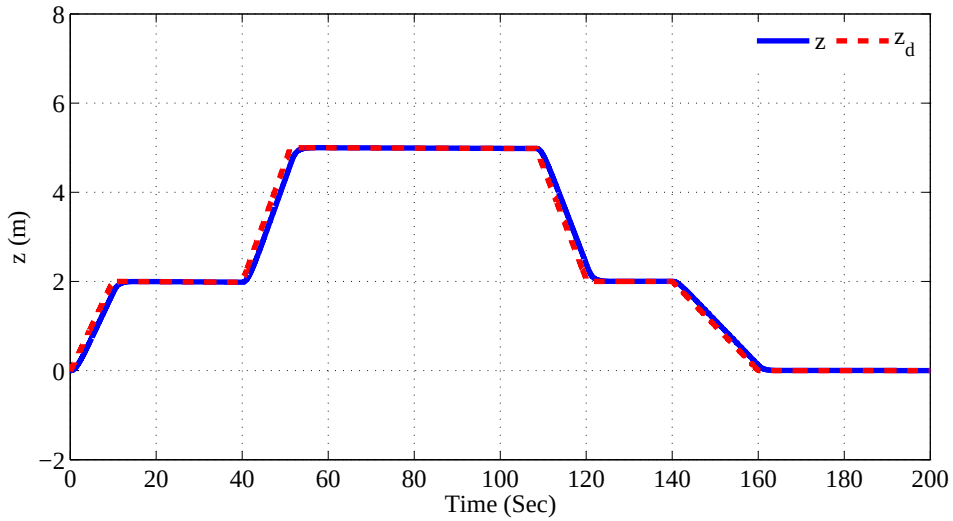

FIGURE 4.26: Depth control with SMC

4.2.8 Circular reference in xz-plane

A circular reference was also provided to the AUV to check its accuracy. The results are shown in Figure 4.33 and Figure 4.34. The vehicle initial starting point was set at x=4m and z=3m

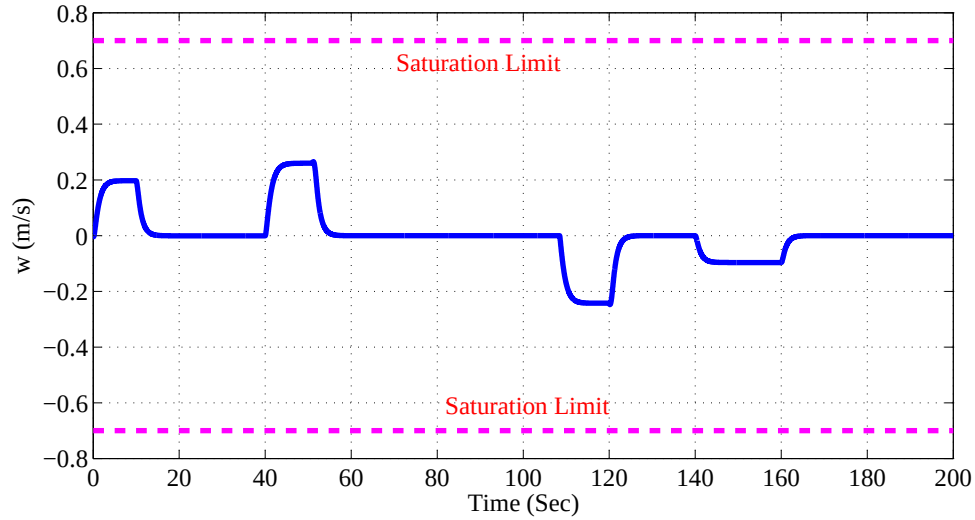

FIGURE 4.27: Heave velocity of KAMBARA

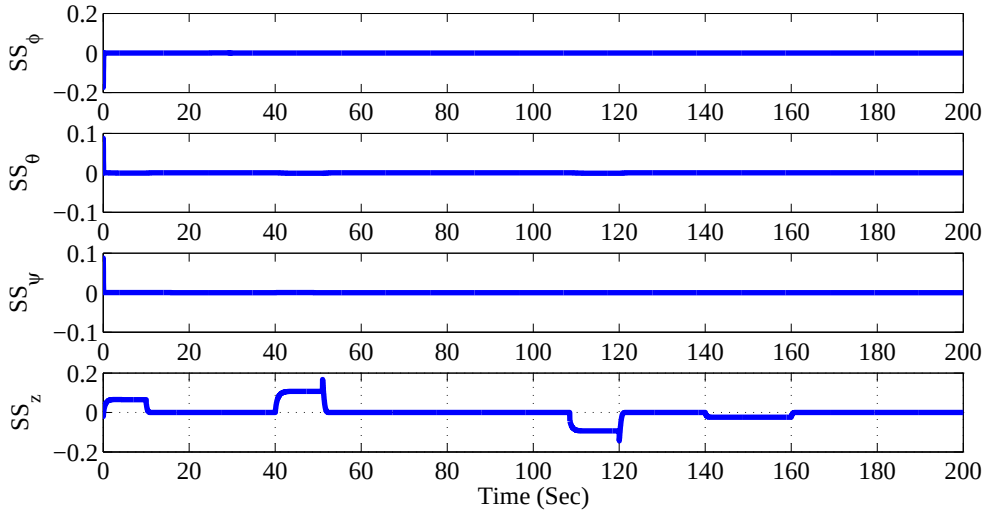

FIGURE 4.28: Sliding surfaces for $\phi, \theta, \psi, z(depth)$with SMC

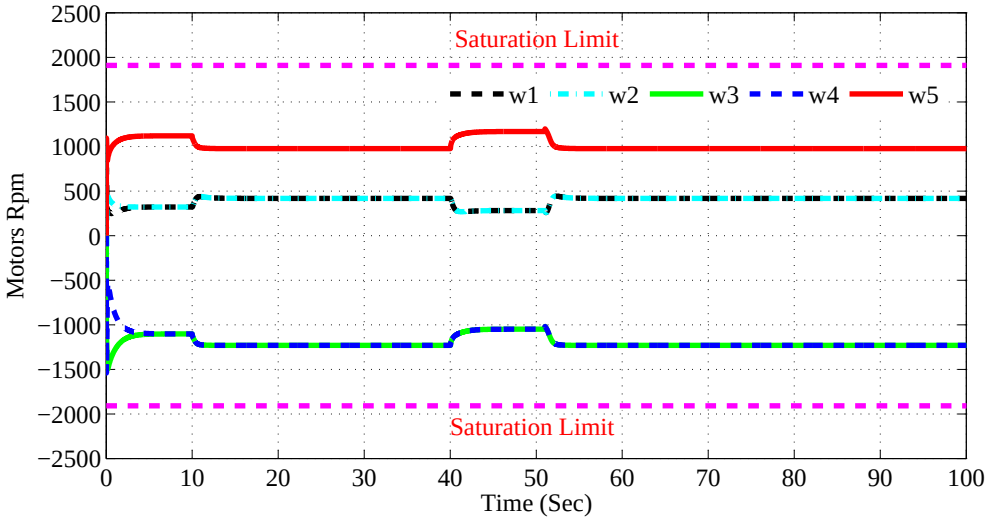

FIGURE 4.29: Motor rpm generated for combined control with SMC

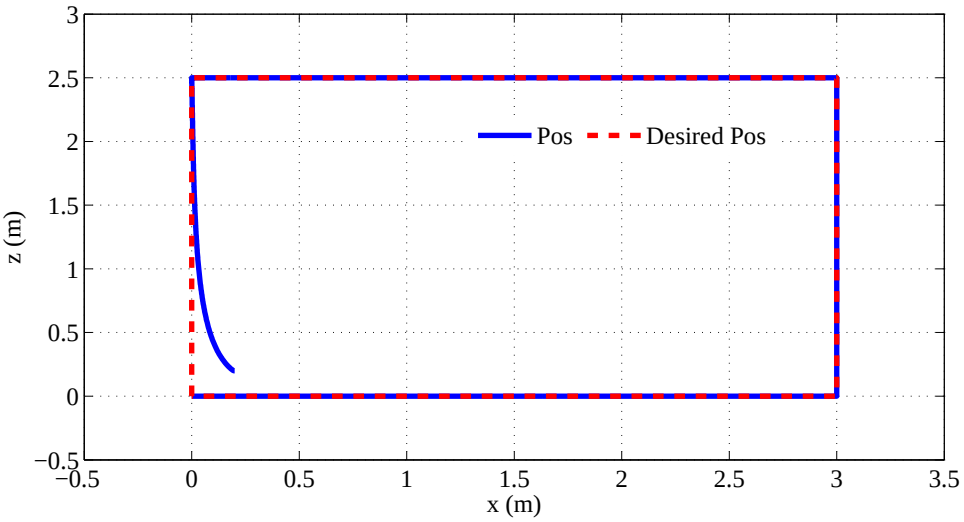

FIGURE 4.30: close-loop mission in xz-plane with SMC

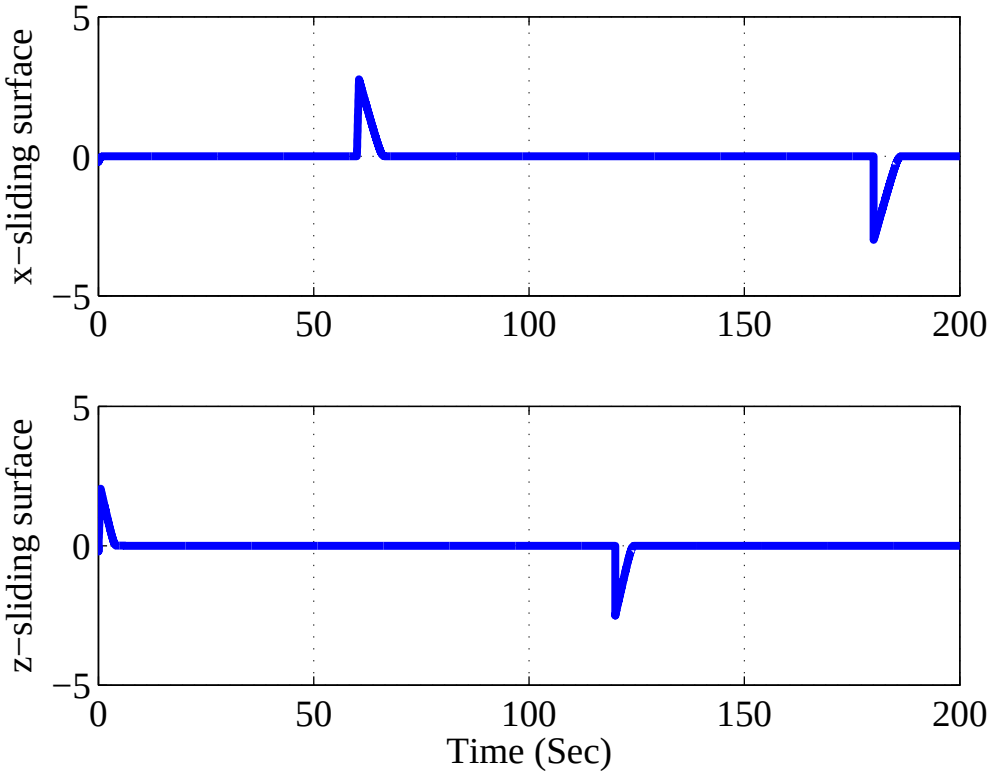

FIGURE 4.31: sliding surface of x and z with SMC

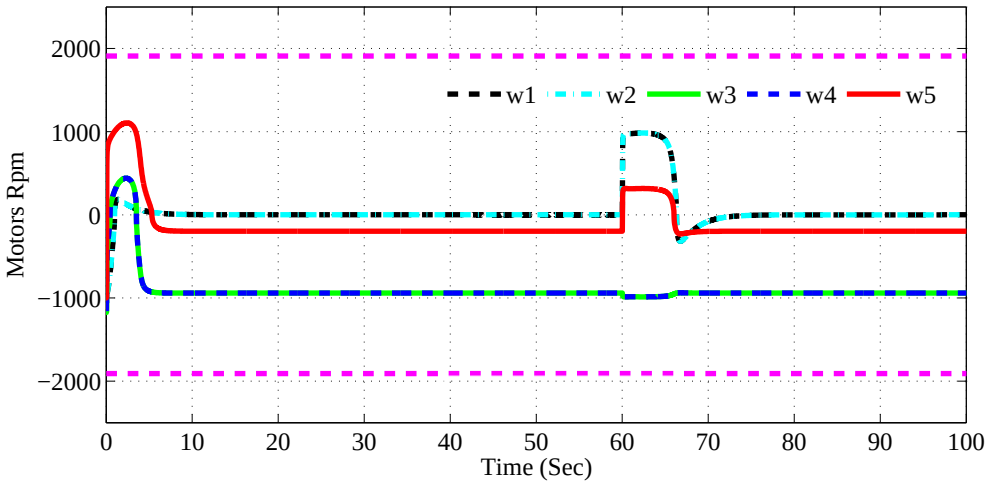

FIGURE 4.32: Motors rpm generated with SMC for closed loop mission

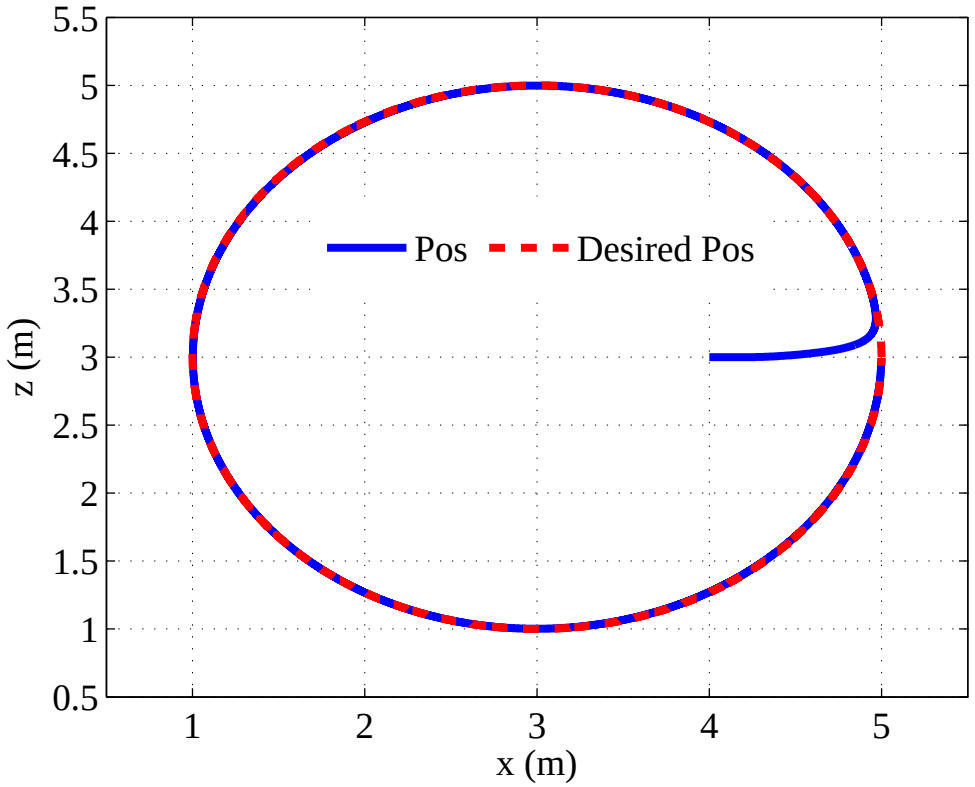

FIGURE 4.33: Circular reference in xz-plane with SMC

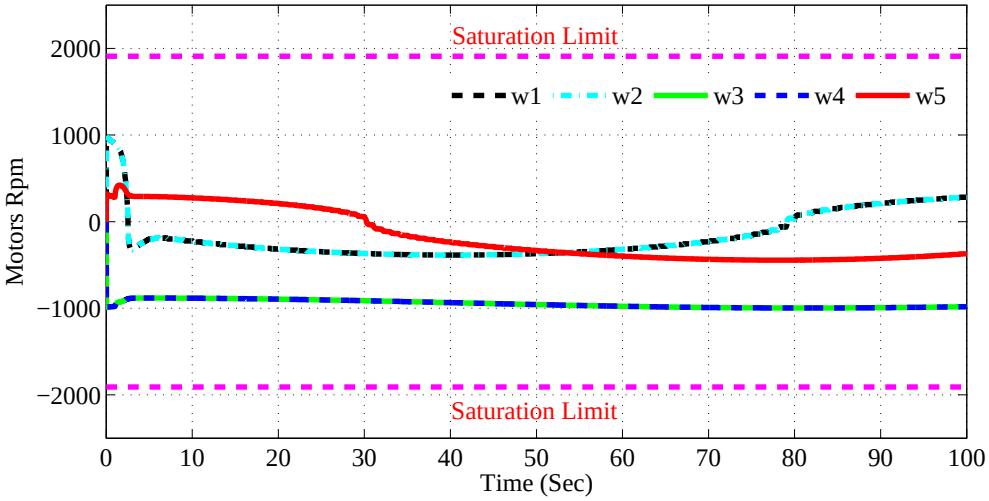

FIGURE 4.34: Motors rpm generated by SMC for circular reference

4.3 Performance Comparison of PID and SMC

This section discusses the performance comparison of the SMC and PID controller designed for KAMBARA AUV. The separate control has already been discussed in section 4.2 and section 4.1, this section discusses the results of the designed controllers plotted simultaneously.

4.3.1 Depth Control

The results for depth control of the vehicle are shown in figure 4.35 where the red line (dashed) is the reference. From the result we see that SMC (solid line) follows the system quite smoothly with no overshoot, while the PID (Dash-dot line) gives a high overshoot and settling time. From the simulation results it is depicted that SMC provides a good overall response as compared with PID.

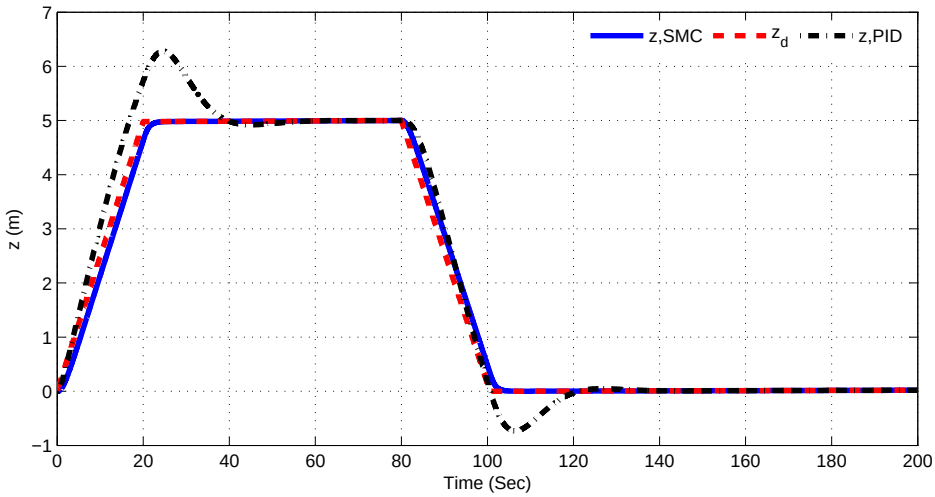

FIGURE 4.35: Depth control comparison of SMC and PID

4.3.2 Roll Control

By providing a reference of 0.35 rad in roll DOF, performance of SMC and PID was compared. PID tends to oscillate at initial start position and then converges to the desired reference angle. The behavior of SMC can be seen to be quite smooth

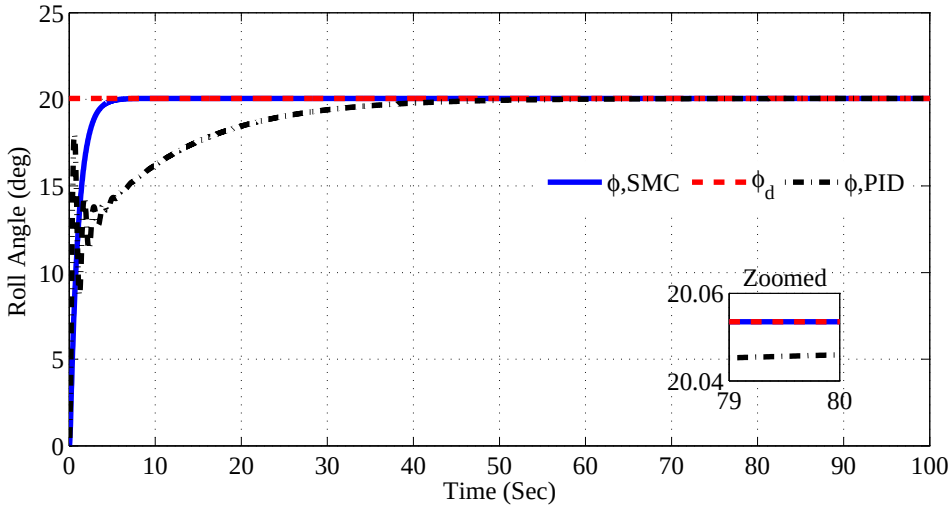

FIGURE 4.36: Performance comparison of SMC and PID for roll control

and quick, shown in figure 4.36. The zoomed portion indicates the accuracy of SMC in terms of steady state error, which is better compared with PID.

	PID	SMC
t_r	15.878s	2.012s
t_s	78s	10s
μ_p	0%	0 %

TABLE 4.1: Performance comparison of SMC and PID for roll control

4.3.3 Combined Control of Pitch, Roll, Psi and Depth

The combined control for PID and SMC was discussed in 4.1.5 and 4.2.6. This section discusses the performance comparison of both controllers shown in Figures 4.37-4.40. The Figures for the control of the desired DOF are plotted separately so that we can analyze the results easily. From the simulation result it is quite prominent that the results of SMC are more better and robust than PID. It was discussed that the 5 DOF for KAMBARA are coupled in terms of the input and it can be seen in Figure 4.38 and Figure 4.37. For PID the coupling effect in terms of depth and pitch are quite prominent while the SMC removes that effect which can be seen in Figure 4.38. It can be also seen that the t_s for PID is 30s, while

SMC has about 7s in terms of yaw control. Also we do not have any overshoot for SMC in terms of depth control.

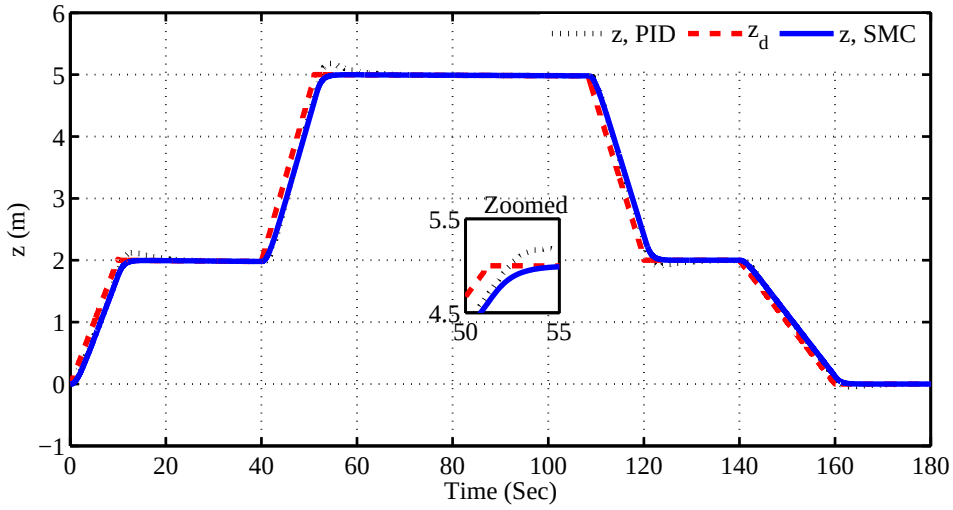

FIGURE 4.37: Performance comparison of SMC and PID (Depth result)

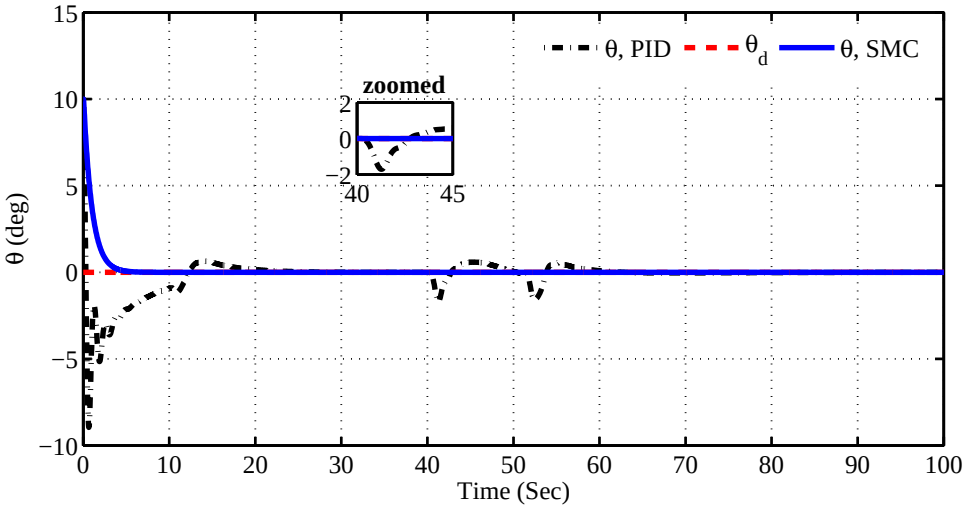

FIGURE 4.38: Performance comparison of PID and SMC (Pitch control)

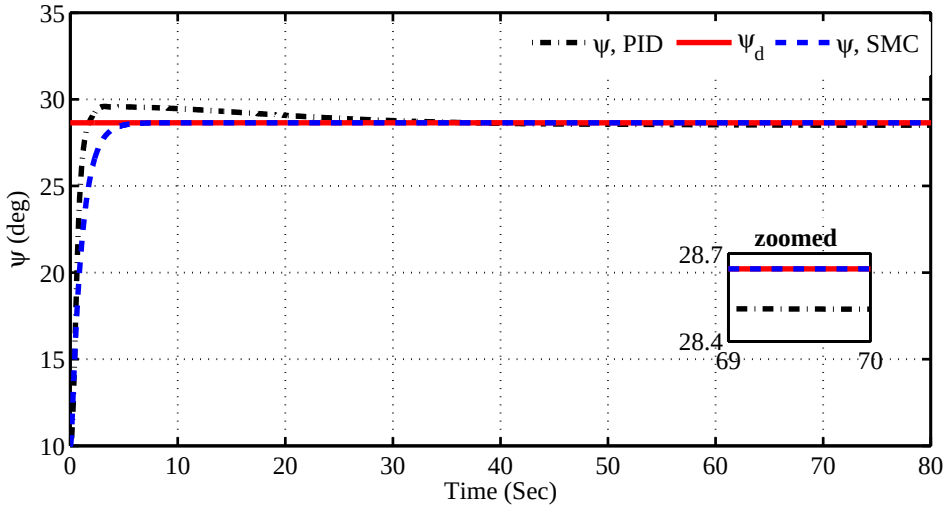

FIGURE 4.39: Performance comparison of PID and SMC (Yaw control)

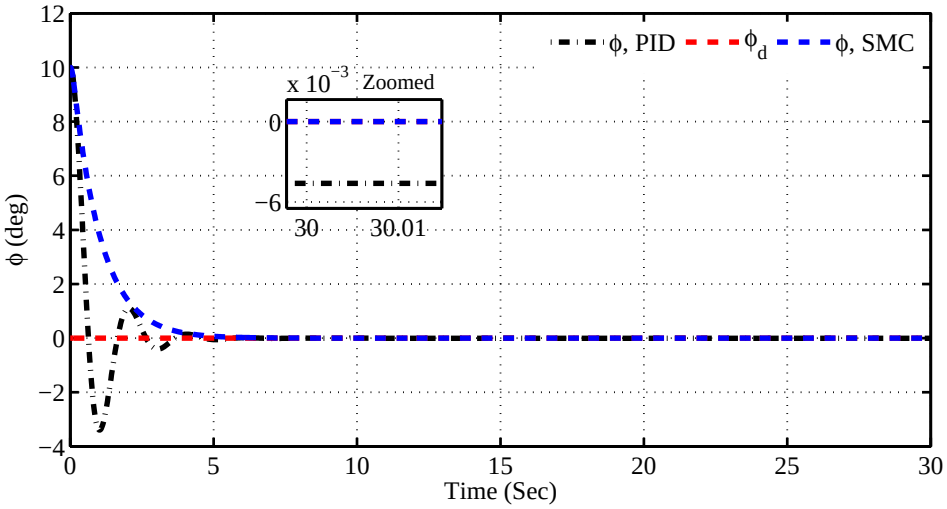

FIGURE 4.40: Performance comparison of PID and SMC (Roll control)

4.4 Performance Comparison of PID and SMC in presence of ocean currents

Mathematical model for ocean currents have already been discussed in chapter 3. Using the knowledge of the model, the performance of the designed SMC and PID controller are analyzed in presence of ocean currents. The controller performance

was studied first using 2D ocean currents followed by 3D ocean currents.

4.4.1 Performance with 2D ocean currents

2D ocean currents were applied to KAMBARA with a side slip angle of 10 deg and current speed of 0.5 m/s. The performance was compared for yaw and roll control of the vehicle using PID and SMC. It is observed that the response of PID for yaw control to the ocean currents is very slow, not able to track reference to a time of 100s. The same reference is achieved by SMC in about 7s canceling the effect of ocean currents, Figure 4.41.

For roll control the same is observed that PID performance is affected in the presence of ocean currents while SMC rejects the effect of currents quite accurately, Figure 4.42. Though it may increase the control input in both the cases

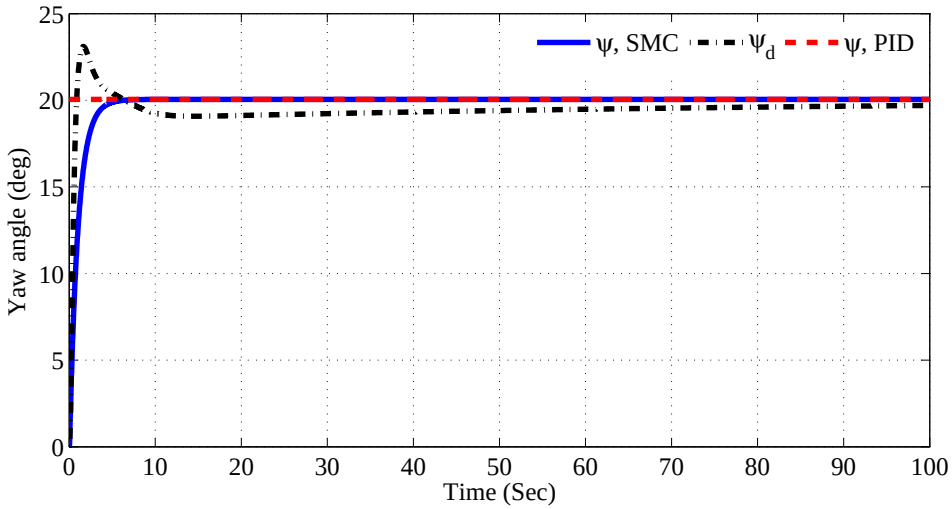

FIGURE 4.41: Performance comparison of Yaw for PID and SMC in presence of ocean currents

4.4.2 Performance with 3D ocean currents

In presence of 3D ocean currents the performance of the designed controllers was analyzed for the circular trajectory in the xz-plane. The speed of ocean current was kept constant at 0.6 m/s. The angle of the ocean current on the vehicle was

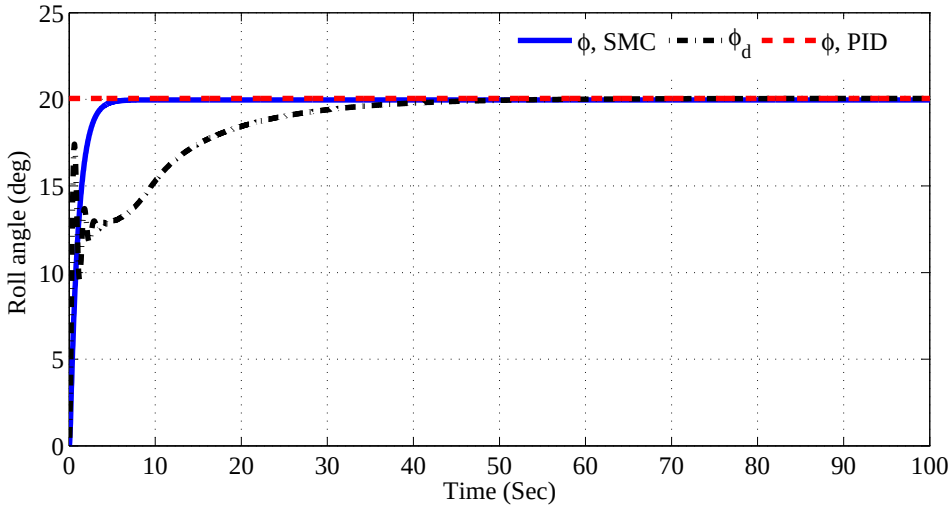

FIGURE 4.42: Performance comparison of Roll for PID and SMC in presence of ocean currents

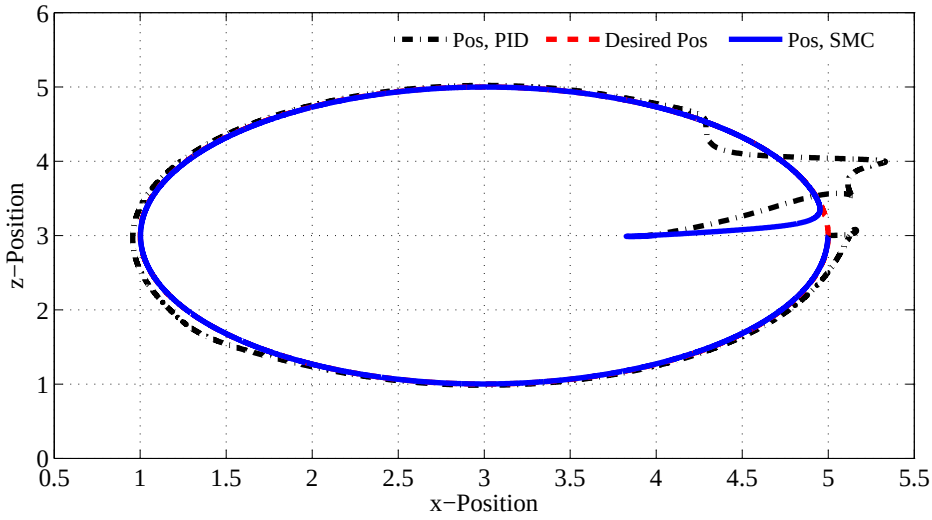

FIGURE 4.43: Performance comparison of SMC and PID in presence of ocean currents (Circular trajectory in xz-plane)

α_c=10 deg and β_c=20 deg. It was observed that SMC was quite robust against the applied currents while PID followed some performance degradation as shown in Figure 4.43

Chapter 5

CONCLUSIONS AND FUTURE RECOMMENDATION

5.1 Conclusions

A mathematical model for Autonomous under water vehicle has been presented in the thesis with the study of the factors that may effect the model. It have been shown that the mathematical model for AUV is a highly coupled non-linear, six DOF model.

KAMBARA AUV was selected to perform the open loop simulation using MATLAB/ SIMULINK. The parameters used for the open loop simulation are disused in chapter 03. The initial simulations also confirms that the vehicle weight is greater than the buoyancy, also the COG and COB are not aligned resulting in a pitch angle .

Using the KAMBARA AUV the thesis objective was to design a controller for depth, roll, pitch, yaw and x-translation. The first controller designed was PID and results were discussed in chapter 04. Due to the non linearity and uncertainty in the dynamic model a Robust controller was needed for KAMBARA. A SMC was considered with comparison of its results with the devised PID controller. It was shown that SMC provided more accurate, disturbance free steady state tracking as compared with the PID

As discussed before Ocean current are one of the major factor that effect motion of AUV, it was desired to check the performance of the designed controller in the presence of ocean currents. Looking to the results it can be deducted that the effect of ocean currents was well rejected by SMC, while PID performance was degraded in the presence of ocean currents.

The overall work can be summarized that for Autonomous Under water vehicle a Sliding mode control can be a good choice in the presence of uncertainties and disturbances.

5.2 Future Work

The work carried out in this thesis can be extended in several ways. A benchmark has been laid down which can be extended to enrich the performance of the vehicle. Work is required to device control in the sway DOF for KAMBARA. Practical implementation of the designed controllers is needed on the vehicle. The thesis had covered the effect of ocean currents on the AUV motion, it is recommended that other disturbance parameters may also be included for the improvement of overall performance of KAMBARA vehicle.

REFERENCES

[1] I.Khan. Control of lateral dynamics of autonomous under water vehicle. Master's thesis, Faculty of Engineering,Muhammad Ali Jinnah University, Islamabad, 2012.

[2] https://www.kongsberg.com/. .

[3] http://www.slideshare.net/hydrographicsocietybnl/km-au-vs-for-benelux-hydrographic society. , 2014.

[4] http://www.apl.washington.edu/project/project.php?id=seaglider. .

[5] http://www.cpmais.com/auv/bluefin auvs/?lang=en. .

[6] Özgür Yildiz, R Bülent Gökalp, and A Egemen Yilmaz. A review on motion control of the underwater vehicles. In *Electrical and Electronics Engineering, 2009. ELECO 2009. International Conference on*, pages II–337. IEEE, 2009.

[7] Chen Yang. *Modular modeling and control for autonomous underwater vehicle (AUV)*. PhD thesis, 2008.

[8] L.A.Gonzalez. Design, modelling and control of an autonomous underwater vehicle. Master's thesis, Mobile Robotics Laboratory, Centre for Intelligent Information Processing Systems, School of Electrical, Electronic and Computer Engineering, The University of Western Australia., 2004.

[9] Thor I Fossen. *Guidance and control of ocean vehicles*. John Wiley & Sons Inc, 1994.

[10] Chanop Silpa-Anan. *Autonomous underwater robot: Vision and control*. Citeseer, 2001.

[11] MY Radzak and MR Arshad. Auv controller design and analysis using full-state feedback. 2005.

[12] Abdelkader Chellabi and Meyer Nahon. Feedback linearization control of undersea vehicles. In *OCEANS'93. Engineering in Harmony with Ocean. Proceedings*, pages I410–I415. IEEE, 1993.

[13] Bjorn Jalving. The ndre-auv flight control system. *IEEE Journal of Oceanic Engineering*, 19(4):497–501, 1994.

[14] Seung-Keon Lee, Kyoung-Ho Sohn, Seung-Woo Byun, and Joon-Young Kim. Modeling and controller design of manta-type unmanned underwater test vehicle. *Journal of mechanical science and technology*, 23(4):987–990, 2009.

[15] Przemysław Herman. Decoupled pd set-point controller for underwater vehicles. *Ocean Engineering*, 36(6):529–534, 2009.

[16] K Küçük. *Modeling and motion Simulation of an Underwater Vehicle*. PhD thesis, MS thesis, Dept. Mech. Eng., Middle East Technical Univ., Ankara, Turkey, 2007.

[17] Sabiha A Wadoo, Sadiksha Sapkota, and Keerthish Chagachagere. Optimal control of an autonomous underwater vehicle. In *Systems, Applications and Technology Conference (LISAT), 2012 IEEE Long Island*, pages 1–6. IEEE, 2012.

[18] W Naeem, Robert Sutton, and John Chudley. System identification, modelling and control of an autonomous underwater vehicle. In *Manoeuvring and Control of Marine Craft 2003 (MCMC 2003): A Proceedings Volume from the 6th IFAC Conference, Girona, Spain, 17 19 September 2003*, 2004.

[19] Ahmad Forouzan Tabar, Mohammad Azadi, and Alireza Alesaadi. Sliding mode control of autonomous underwater vehicles. *World Academy of Science, Engineering and Technology, International Journal of Computer, Electrical, Automation, Control and Information Engineering*, 8(3):546–549, 2015.

[20] Thor I Fossen and Svein I Sagatun. Adaptive control of nonlinear underwater robotic systems. In *Robotics and Automation, 1991. Proceedings., 1991 IEEE International Conference on*, pages 1687–1694. IEEE, 1991.

[21] T Salgado-Jimenez, J-M Spiewak, Philippe Fraisse, and Bruno Jouvencel. A robust control algorithm for auv: based on a high order sliding mode. In *OCEANS'04. MTTS/IEEE TECHNO-OCEAN'04*, volume 1, pages 276–281. IEEE, 2004.

[22] Ji-Hong Li and Pan-Mook Lee. Design of an adaptive nonlinear controller for depth control of an autonomous underwater vehicle. *Ocean engineering*, 32(17):2165–2181, 2005.

[23] N Kato, Y Ito, J Kojima, and K Asakawa. Guidance and control of autonomous underwater vehicle aqua explorer 1000 for inspection of underwater cables. In *International symposium on unmanned untethered submersible technology*, pages 195–195. University of new Hampshire-Marine Systems, 1993.

[24] A Pedro Aguiar, Joao P Hespanha, et al. Trajectory-tracking and path-following of underactuated autonomous vehicles with parametric modeling uncertainty. *IEEE Transactions on Automatic Control*, 52(8):1362–1379, 2007.

[25] Tae Kyu Ha, Eko Henfri Binugroho, Young Bong Seo, and Jae Weon Choi. Sliding mode control for autonomous underwater vehicle under open control platform environment. In *SICE Annual Conference, 2008*, pages 1345–1350. IEEE, 2008.

[26] Halil Akçakaya, H Alpaslan Yildiz, Gaye Sağlam, and Fuat Gürleyen. Sliding mode control of autonomous underwater vehicle. In *Electrical and Electronics Engineering, 2009. ELECO 2009. International Conference on*, pages II–332. IEEE, 2009.

[27] Ahmad Forouzan Tabar, Mohammad Azadi, and Alireza Alesaadi. Sliding mode control of autonomous underwater vehicles. *World Academy of Science, Engineering and Technology, International Journal of Computer, Electrical, Automation, Control and Information Engineering*, 8(3):546–549, 2015.

[28] Yoong Siang Song and Mohd Rizal Arshad. Sliding mode depth control of a hovering autonomous underwater vehicle. In *Control System, Computing and Engineering (ICCSCE), 2015 IEEE International Conference on*, pages 435–440. IEEE, 2015.

[29] Jongan Lee, Mootaek Roh, Jinsung Lee, and Doheon Lee. Clonal selection algorithms for 6-dof pid control of autonomous underwater vehicles. In *Artificial Immune Systems*, pages 182–190. Springer, 2007.

[30] Thomas R Kane, Peter W Likins, and David A Levinson. Spacecraft dynamics. *New York, McGraw-Hill Book Co, 1983, 445 p.*, 1, 1983.

[31] D Grosset, JV Catret Mascarell, F Andritsos, and C Papadopoulos. Quasi-rigid docking of auv for underwater manipulations. In *Proceedings of the 4th International Workshop on Computer Science and Information Technologies*, 2002.

[32] Odd Faltinsen. *Sea loads on ships and offshore structures*, volume 1. Cambridge university press, 1993.

[33] Side Zhao. *Advanced control of autonomous underwater vehicles*. PhD thesis, UNIVERSITY OF HAWAI'I, 2004.

[34] Michael V Jakuba. *Modeling and control of an autonomous underwater vehicle with combined foil/thruster actuators*. PhD thesis, Massachusetts Institute of Technology and Woods Hole Oceanographic Institution, 2003.

[35] Ola-Erik Fjellstad. Control of unmanned underwater vehicles in six degrees of freedom: a quaternion feedback approach. *Dr. ing. thesis, Norwegian Institute of Technology, Norway*, 1994.

[36] Ola-Erik Fjellstad and Thor I Fossen. Position and attitude tracking of auv's: a quaternion feedback approach. *Oceanic Engineering, IEEE Journal of*, 19(4):512–518, 1994.

[37] TI Fossen and A Ross. Nonlinear modelling, identification and control of uuvs. *IEE Control Engineering Series*, 69:13, 2006.

[38] E Omerdic and D Toal. Modelling of waves and ocean currents for real-time simulation of ocean dynamics. In *OCEANS 2007-Europe*, pages 1–6. IEEE, 2007.

[39] Sohail Iqbal, Aamer Iqbal Bhatti, and Qadeer Ahmed. Dynamic analysis and robust control design for stewart platform with moving payloads. *IFAC Proceedings Volumes*, 41(2):5324–5329, 2008.

[40] Jean-Jacques E Slotine, Weiping Li, et al. *Applied nonlinear control*, volume 199. prentice-Hall Englewood Cliffs, NJ, 1991.